Dynamic flows of grains … and powders?

Nico Gray, Department of Mathematics, The University of Manchester, UK

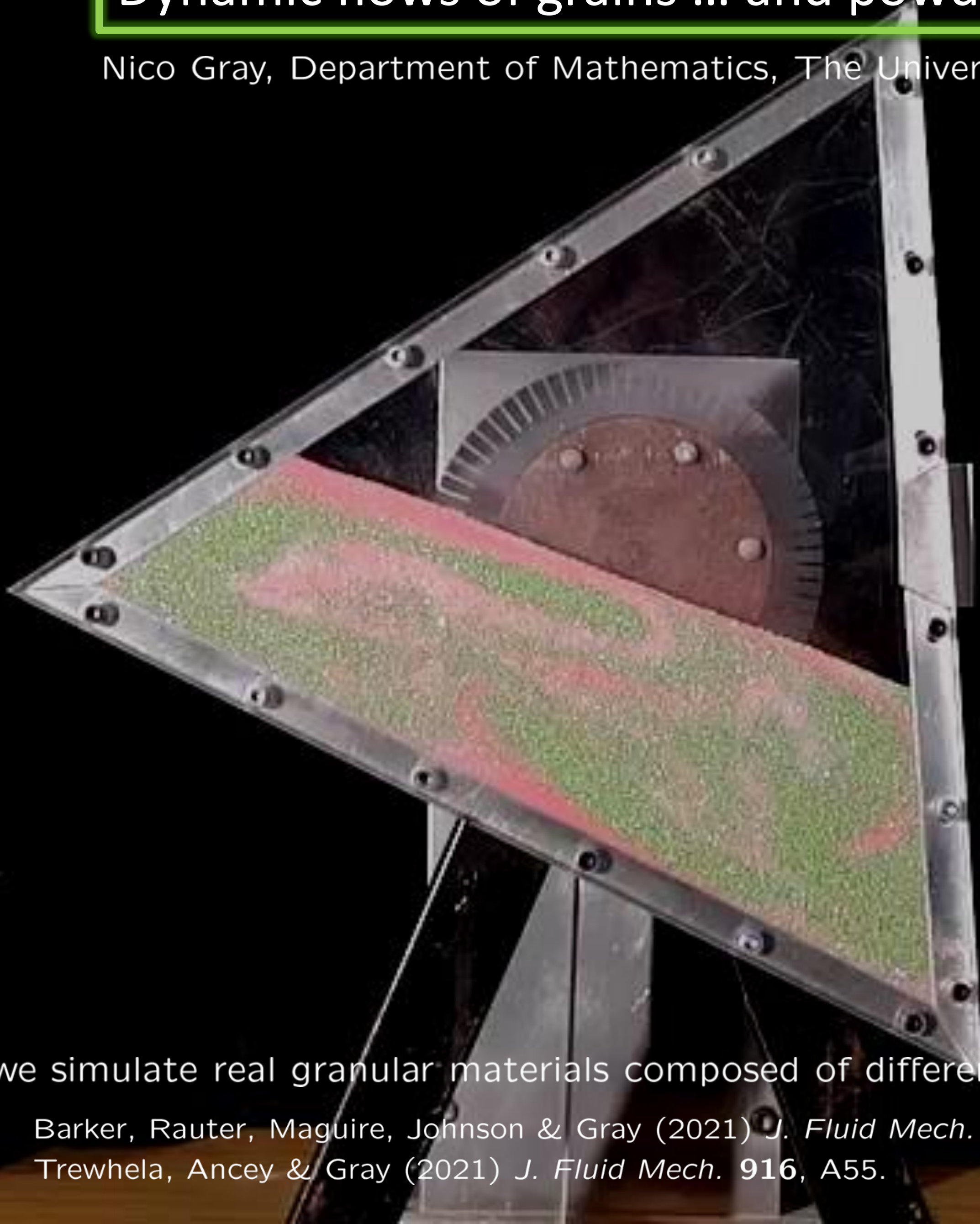

500–750 μm
400–500 μm
75–150 μm

- Can we simulate real granular materials composed of differently sized particles?

Barker, Rauter, Maguire, Johnson & Gray (2021) *J. Fluid Mech.* **909**, A22.
Trewhela, Ancey & Gray (2021) *J. Fluid Mech.* **916**, A55.

The $\mu(I)$-rheology and the $\mu(I),\Phi(I)$-rheology for dry grains

Savage, S. B. 1984 *Advances in Applied Mechanics*, **24**, 289366
GDR MiDi (2004) *Eur. Phys. J. E* **14**, 341-365.

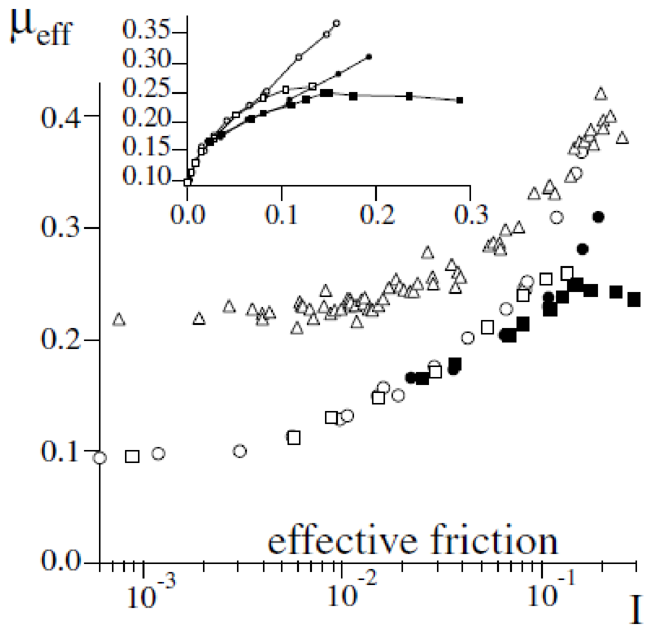

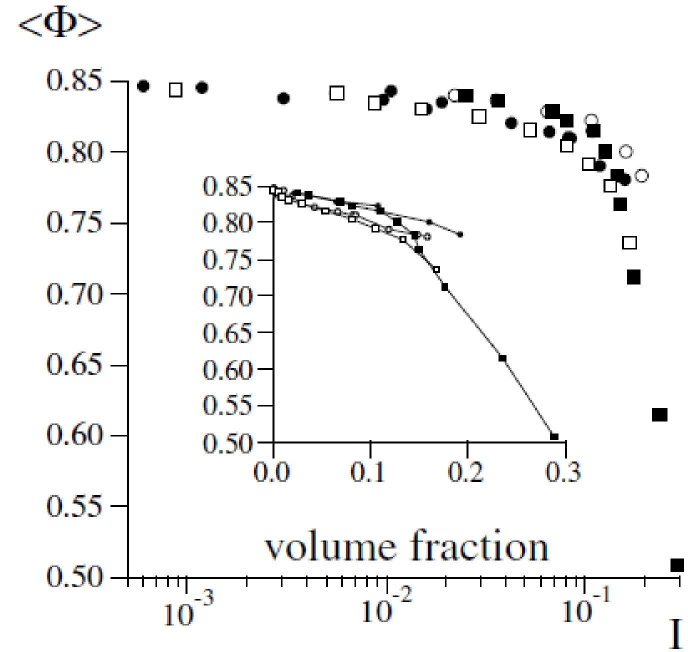

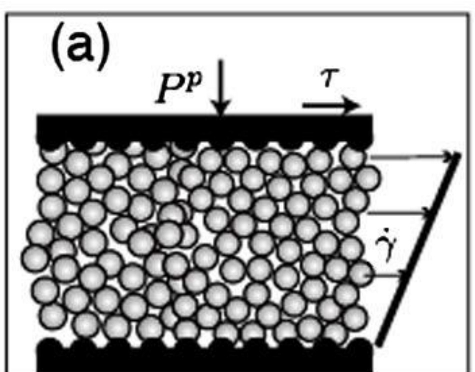

Simple shear experiment

$$\tau = \mu(I)P, \quad \phi = \phi(I), \quad I = \frac{\dot{\gamma} d}{\sqrt{P/\rho}}$$

where τ is the shear stress, P is pressure, ϕ is the solids volume fraction, $\dot{\gamma}$ is the shear-rate, d is the particle size, ρ is the density and I is the dimensionless inertial number

The tensorial form of the incompressible $\mu(I)$-rheology

Jop, Forterre & Pouliquen (2006) *Nature* **441**, 727-730.

Cauchy stress $\boldsymbol{\sigma}$ is decomposed into a pressure p and deviatoric stress $\boldsymbol{\tau}$

$$\boldsymbol{\sigma} = -p\mathbf{1} + \boldsymbol{\tau}$$

The tensorial form of the incompressible $\mu(I)$-rheology is

$$\boldsymbol{\tau} = \mu(I)p\frac{\boldsymbol{D}}{||\boldsymbol{D}||}, \quad \text{or} \quad \boldsymbol{\tau} = 2\eta\boldsymbol{D}, \quad \text{where} \quad \eta = \frac{\mu(I)p}{2||\boldsymbol{D}||}$$

where $\boldsymbol{D}$ is the strain-rate, $||\boldsymbol{D}|| = \dot{\gamma}/2$ is the second invariant

$$||\boldsymbol{D}|| = \sqrt{\frac{1}{2}\mathrm{tr}\boldsymbol{D}^2},$$

and the inertial number

$$I = \frac{2||\boldsymbol{D}||d}{\sqrt{p/\rho}},$$

The $\mu(I)$-curve asymptotes to μ_2 as $I \longrightarrow \infty$

$$\mu(I) = \mu_1 + \frac{\mu_2 - \mu_1}{I_0/I + 1},$$

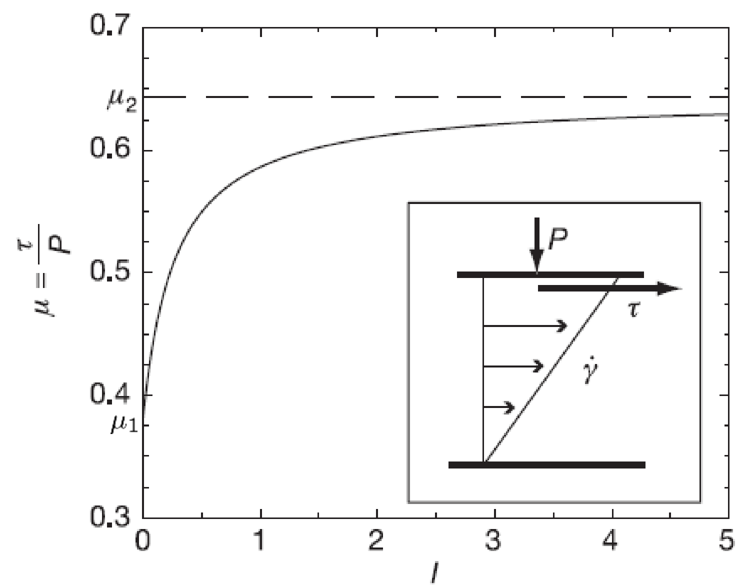

Solver: We apply the Open-source Gerris (Popinet 2003)
http: //gfs.sourceforge.net
(incompressible Navier-Stokes equations using a VOF method) (Popinet 2003, 2009)

$$\begin{aligned}
\boldsymbol{\nabla}.\boldsymbol{u} &= 0 \\
\rho\left(\frac{\partial \boldsymbol{u}}{\partial t} + \boldsymbol{u}.\boldsymbol{\nabla}\boldsymbol{u}\right) &= -\boldsymbol{\nabla}p + \boldsymbol{\nabla}.(2\eta\boldsymbol{D}) + \rho\boldsymbol{g} \\
\frac{\partial c}{\partial t} + \boldsymbol{\nabla}.(c\boldsymbol{u}) &= 0 \\
\rho = c\,\rho_{\mathrm{air}} \; &+ \; (1-c)\,\rho_{\mathrm{grains}} \\
\eta = c\,\eta_{\mathrm{air}} \; &+ \; (1-c)\,\eta_{\mathrm{grains}}
\end{aligned}$$

⇒ We chose $\rho_{\mathrm{air}} << \rho_{\mathrm{grains}}$
⇒ The free surface is solved in the course of time
⇒ We implement the viscosity:

$$\eta_{\mathrm{grains}} = \min\left(\frac{\mu P}{|\dot{\gamma}|}, \eta_{max}\right),$$

Lagree, Staron & Popinet 2011

The Continuum Sand-Glass

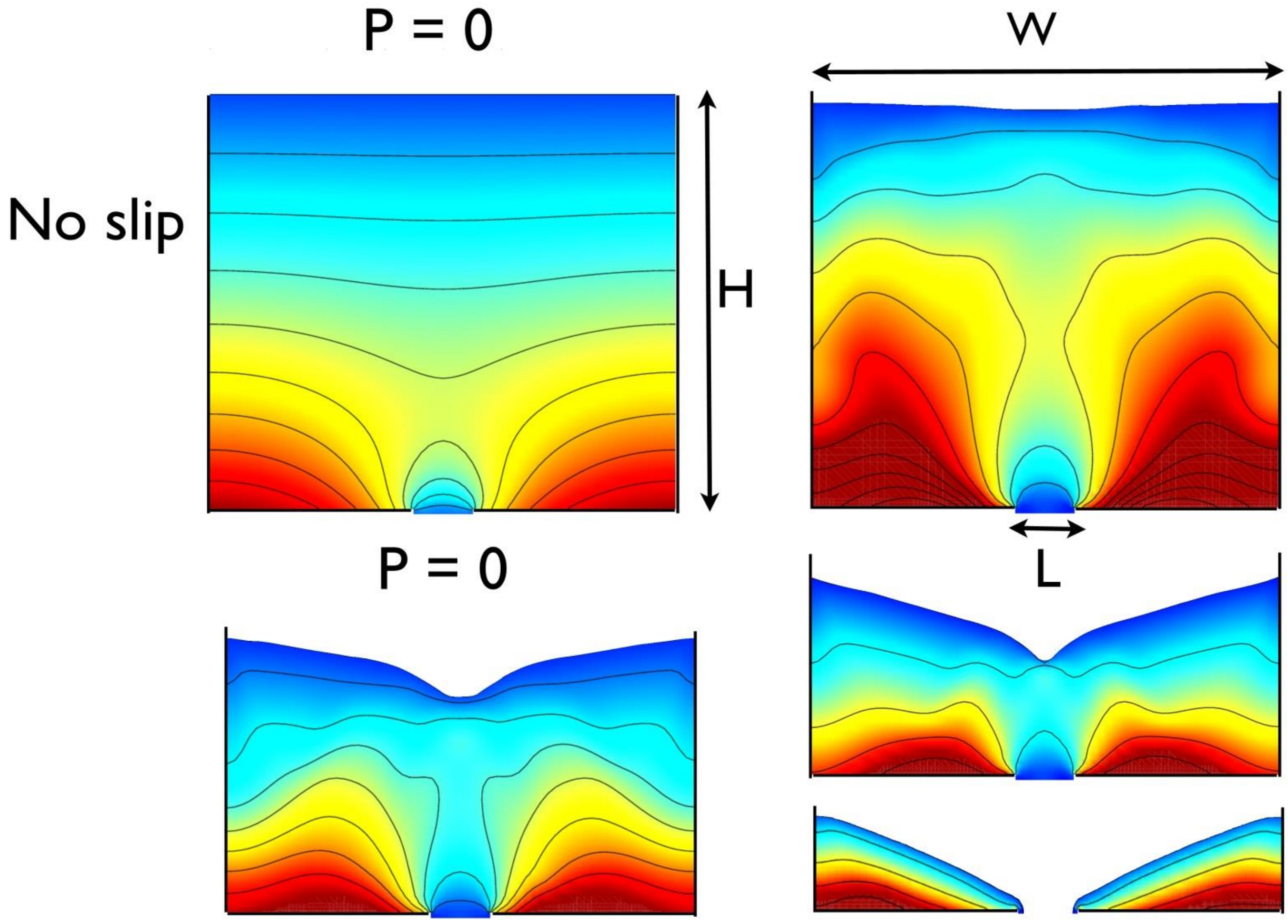

We chose the following value for the rheological parameters:
$\mu_s = 0.32$, $\mu_d = 0.60$, $I_0 = 0.4$

Staron, Lagree & Popinet 2011

JOURNAL OF DIFFERENTIAL EQUATIONS **66**, 19–50 (1987)

BUT, if $\mu =$ constant this reduces to Drucker-Prager plasticity, which is always ill-posed

Instability in the Evolution Equations Describing Incompressible Granular Flow

DAVID G. SCHAEFFER*

Department of Mathematics, Duke University, Durham, North Carolina 27706

Received September 10, 1985

1. INTRODUCTION

In this paper, equations governing the time dependent flow of granular material under gravity are derived and analyzed. Formally these equations bear a strong resemblance to the Navier–Stokes equations for the flow of an incompressible, viscous fluid. However, the main result of this paper is that, depending on geometric and material parameters, the equations governing granular flow may lead to a violent instability analogous to that for

$$u_t = u_{xx} - u_{yy};$$

i.e., in some directions in Fourier transform space, the linearization of the

Well-posed and ill-posed behaviour of the incompressible μ(I)-rheology

Barker, Schaeffer, Bohorquez & Gray (2015) *J. Fluid Mech.* *779*, 794-818.

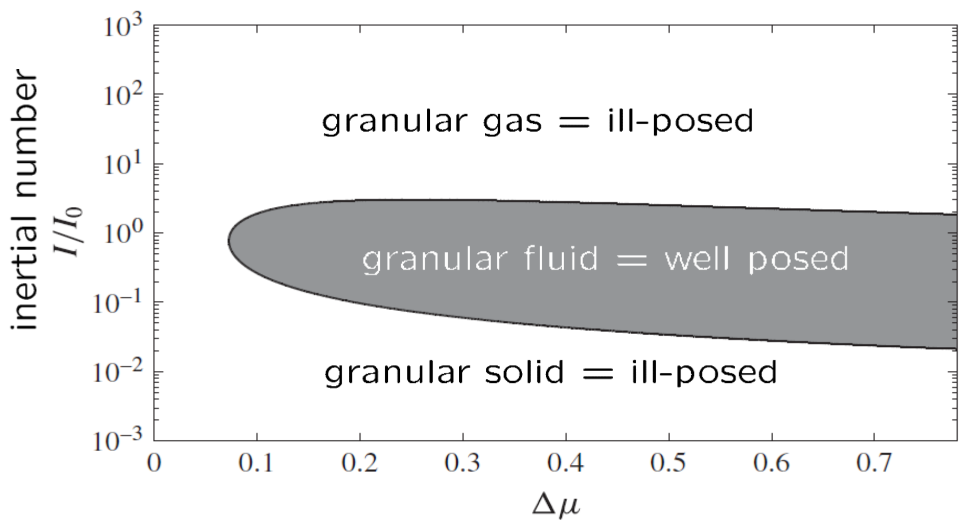

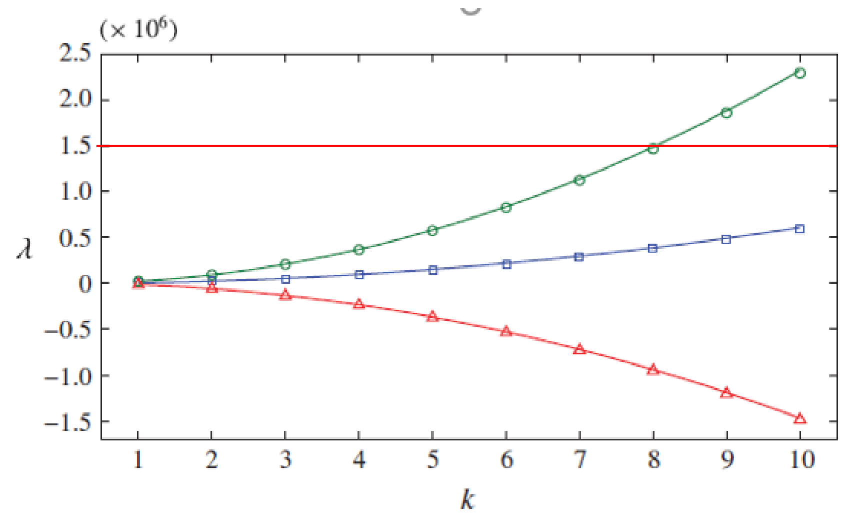

$$\mu(I) = \mu_1 + \frac{\Delta\mu}{I_0/I + 1}$$

- ill-posed directions produce oblique pressure perturbations
- that grow uncontrollably in the high wavenumber limit
- ⇒ grid-size dependent results!

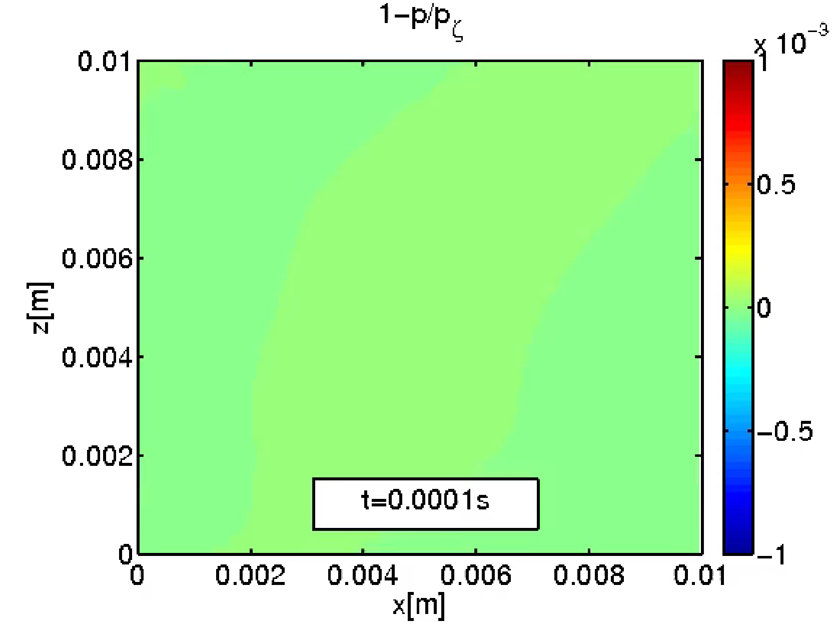

The partially regularized incompressible $\mu(I)$-rheology

The $\mu(I)$-rheology is a good steady-state theory, but it is ill-posed if

$$4\left(\frac{I\mu'}{\mu}\right)^2 - 4\left(\frac{I\mu'}{\mu}\right) + \mu^2\left(1-\frac{I\mu'}{2\mu}\right)^2 > 0, \qquad \text{where} \qquad \mu' = \frac{d\mu}{dI}.$$

This leads to catastrophic instabilities and grid-size dependent results.

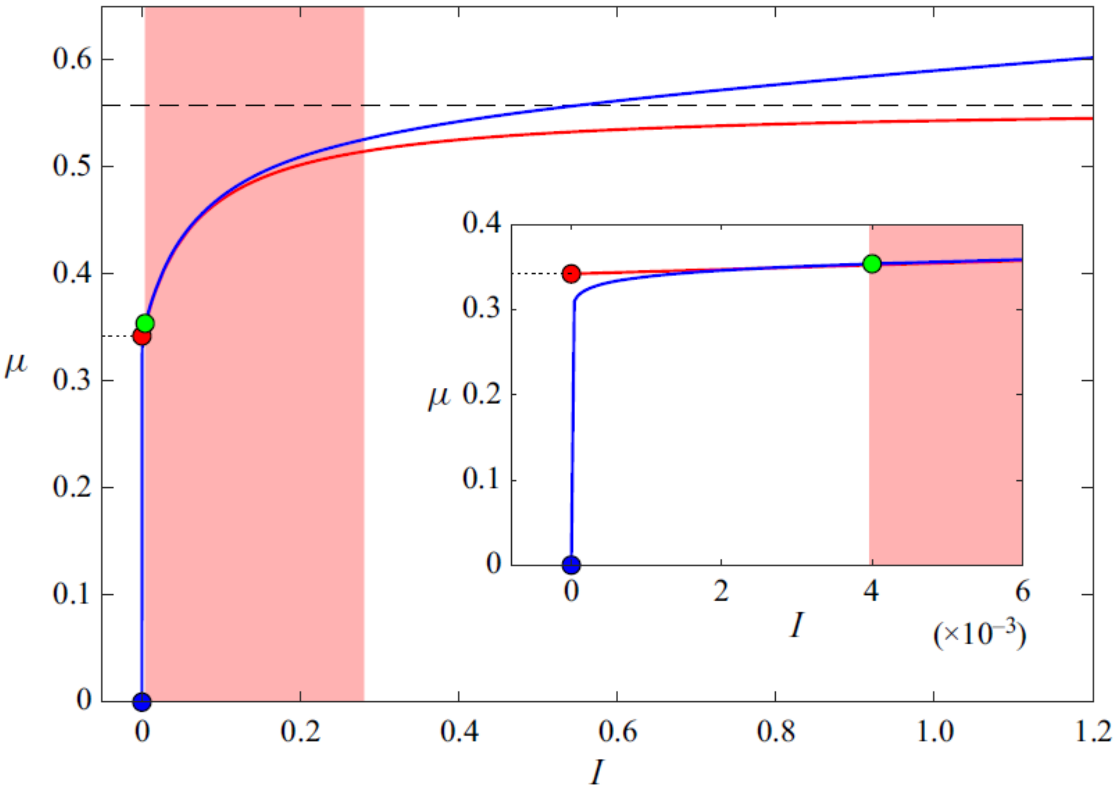

original $\mu(I)$-curve (red)

well-posed in red region

partially regularized curve is well posed $I \in [0, I_{max}]$

- linear for large I
- passes through $\mu(0) = 0$
- introduces a creep state for small I

Barker, Schaeffer, Bohorquez & Gray (2015) *J. Fluid Mech.* **779**, 794-818.

Barker & Gray (2017) *J. Fluid Mech.* **828**, 5–32.

Granular roll waves on an inclined plane

- Steady-uniform flow Bagnold flow for a flow of depth h

$$p = \rho g(h - z)\cos\zeta, \qquad u = \frac{2I_\zeta}{3d}\sqrt{\Phi g \cos\zeta}\left(h^{3/2} - (h - z)^{3/2}\right).$$

- is unstable to perturbations at sufficiently high Froude numbers ...

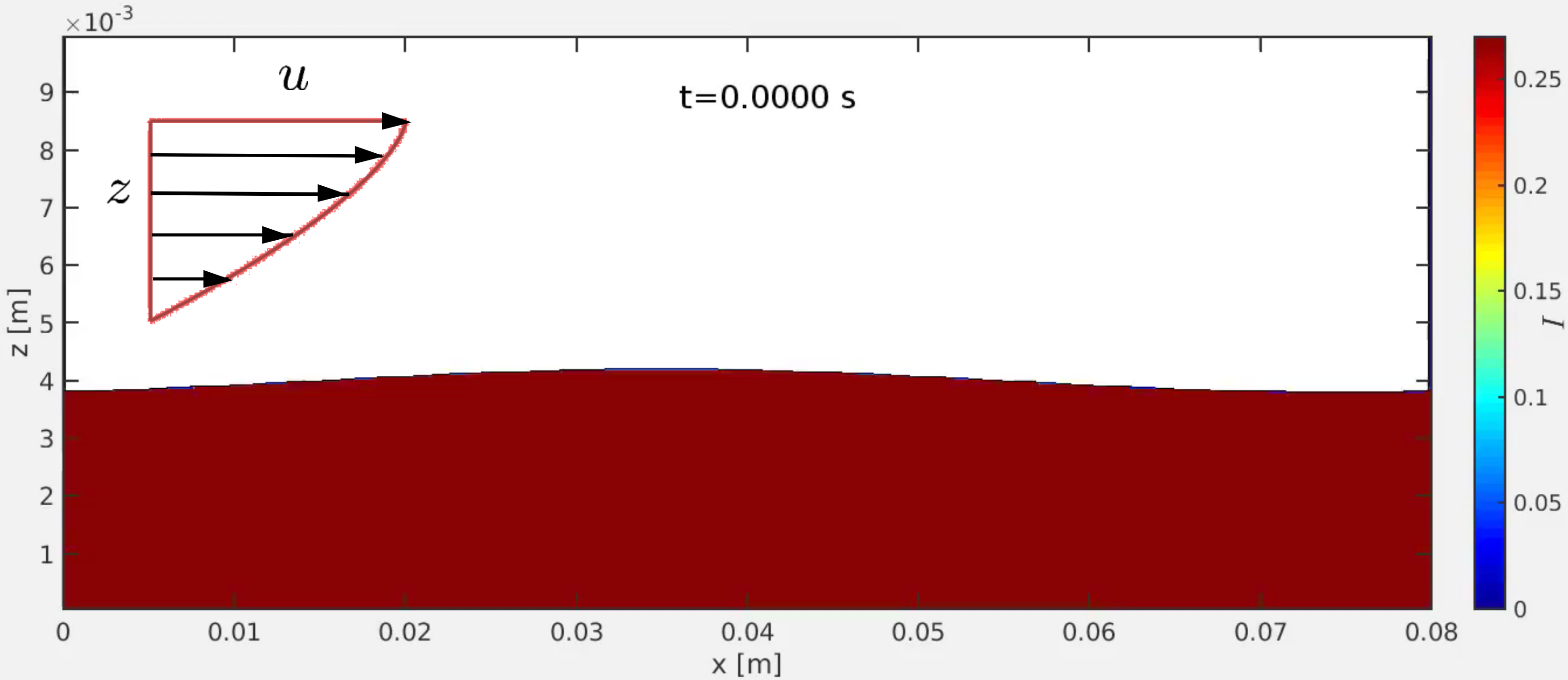

- Numerical solutions do not blow-up and are grid converged

Barker & Gray (2017) *J. Fluid Mech.* **828**, 5–32.

Particle segregation in bidisperse granular flows

- The volume fraction of large and small particles $\phi^l, \phi^s \in [0,1]$ per unit granular volume, satisfy the summation constraint

$$\phi^l + \phi^s = 1, \qquad \Rightarrow \qquad \phi^l = 1 - \phi^s$$

- In an incompressible bulk flow $\boldsymbol{u}$, the small particle concentration satisfies the segregation-advection-diffusion equation

$$\frac{\partial \phi^s}{\partial t} + \nabla \cdot (\phi^s \boldsymbol{u}) + \nabla \cdot \left(f_{sl} \phi^s \phi^l \frac{\boldsymbol{g}}{|\boldsymbol{g}|} \right) = \nabla \cdot (\mathcal{D}_{sl} \nabla \phi^s),$$

where f_{sl} is the segregation velocity magnitude, $\boldsymbol{g}$ is the gravitational acceleration and $\mathcal{D}_{sl}$ is the diffusivity.

- The segregation flux automatically shuts off when $\phi^s = 0, 1$.

- The vertical velocities of the large and small particles are

$$w^l = +f_{sl}\phi^s, \qquad w^s = -f_{sl}\phi^l,$$

as large particles are "squeezed" upwards and small particles percolate downwards under the action of gravity (and shear).

Gray & Thornton (2005) *Proc. R. Soc. A* **461** 1447–1473
Gray & Chugunov (2006) *J. Fluid Mech.* **569**, 365-398.
Gray & Ancey (2011) *J. Fluid Mech.* **678** 535–588
Gray (2018) *Ann. Rev. Fluid Mech.* **50**, 407–433.

Single intruder refractive index matched shear box experiments

Trewhela, Ancey & Gray (2021) *J. Fluid Mech.* **916**, A55.

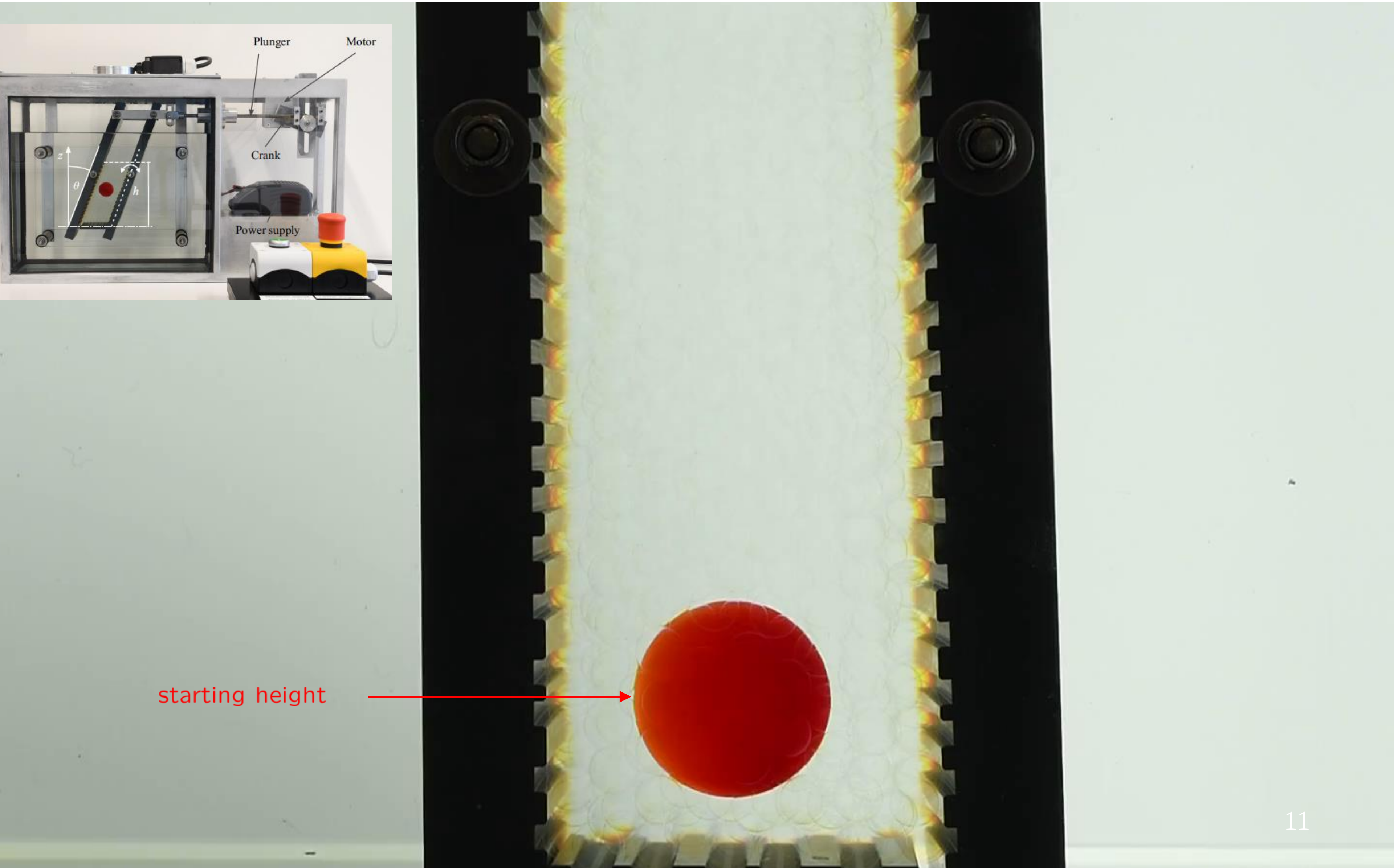

Trajectories of a single large intruder with varying grain size ratio

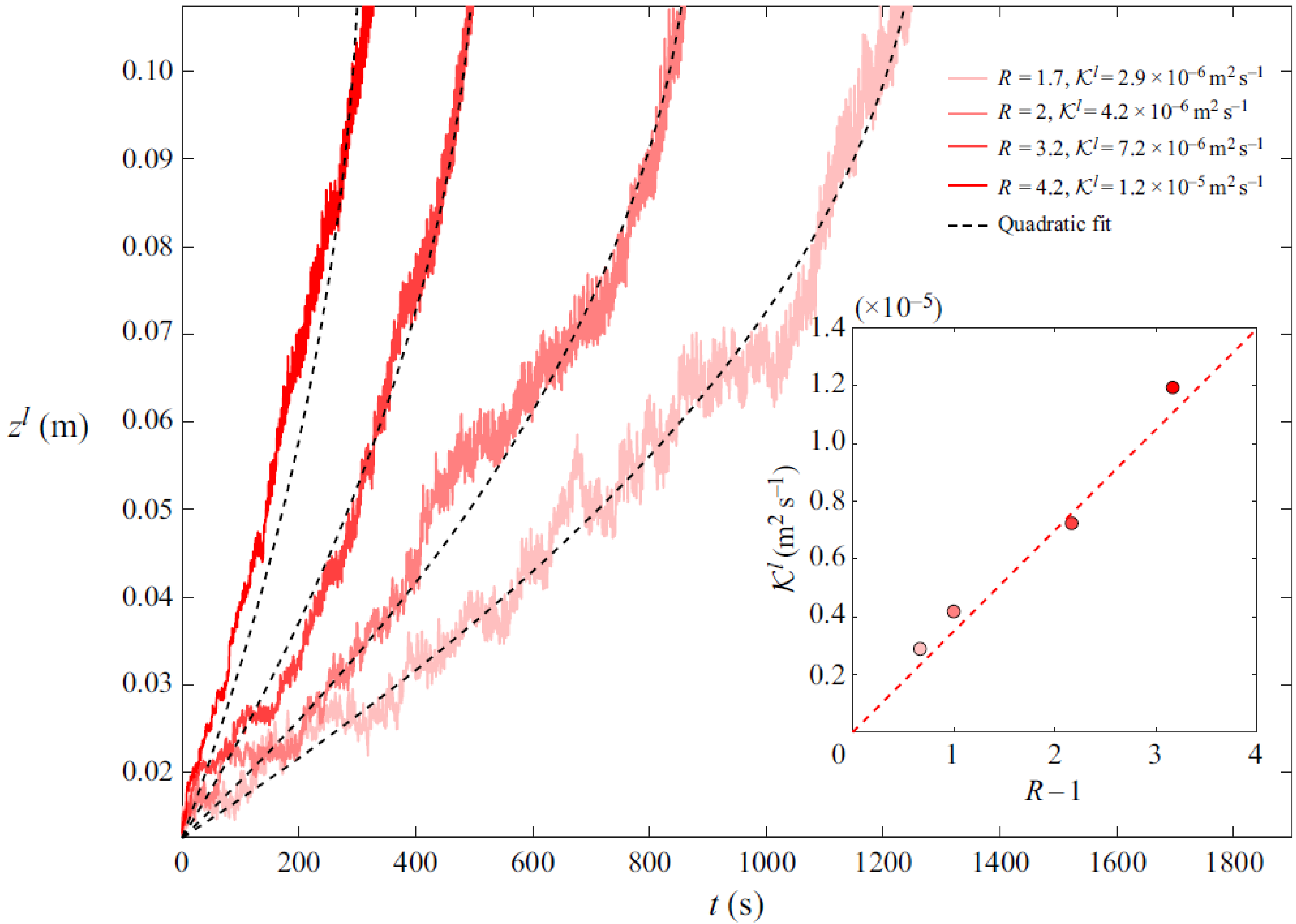

$\Rightarrow$ a linear dependence on the grain-size ratio $R = d^l/d^s$.

- Note the curved trajectories $\Rightarrow$ a p^{-1} pressure dependence.

Trajectories of a single large intruder with varying shear rate

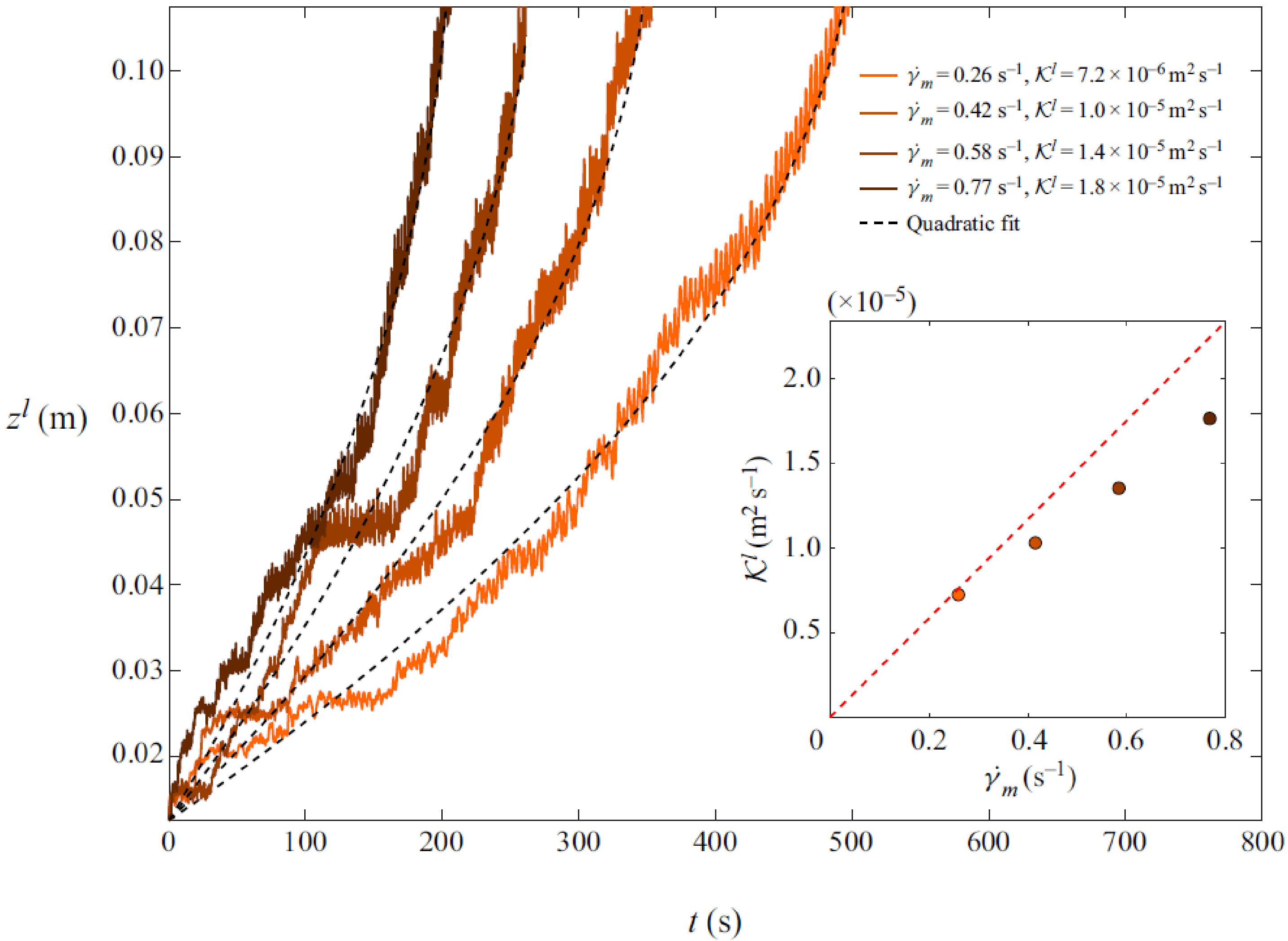

- Suggest a linear dependence on the shear rate $\dot{\gamma} = 2||\boldsymbol{D}||$.

Trewhela, Ancey & Gray (2021) *J. Fluid Mech.* **916**, A55.

Trajectories of a single small intruder with varying shear rate

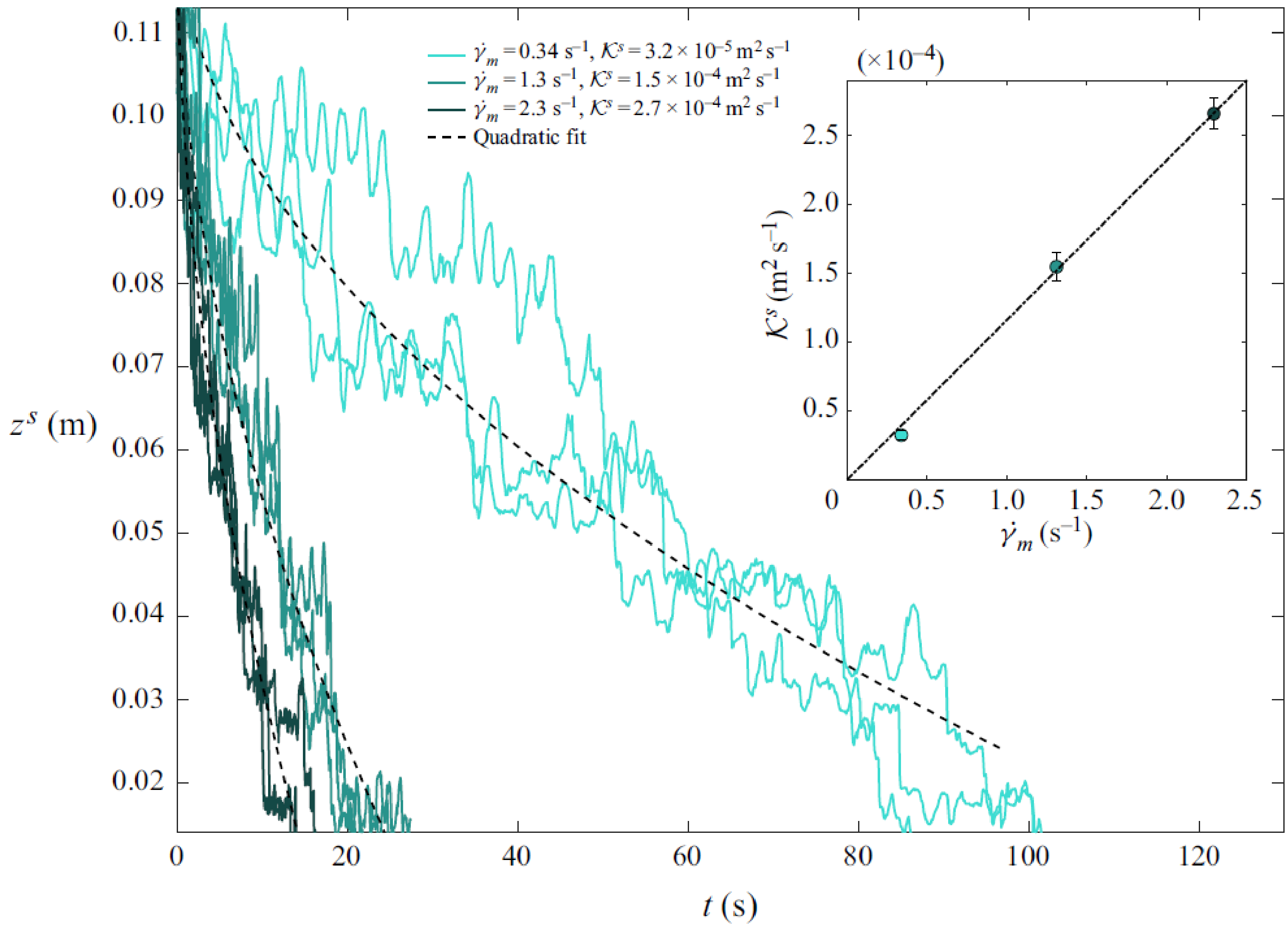

- Are more variable, but also suggest a linear dependence on $\dot{\gamma} = 2||\boldsymbol{D}||$

Trajectories of a single small intruder with varying grain size ratio

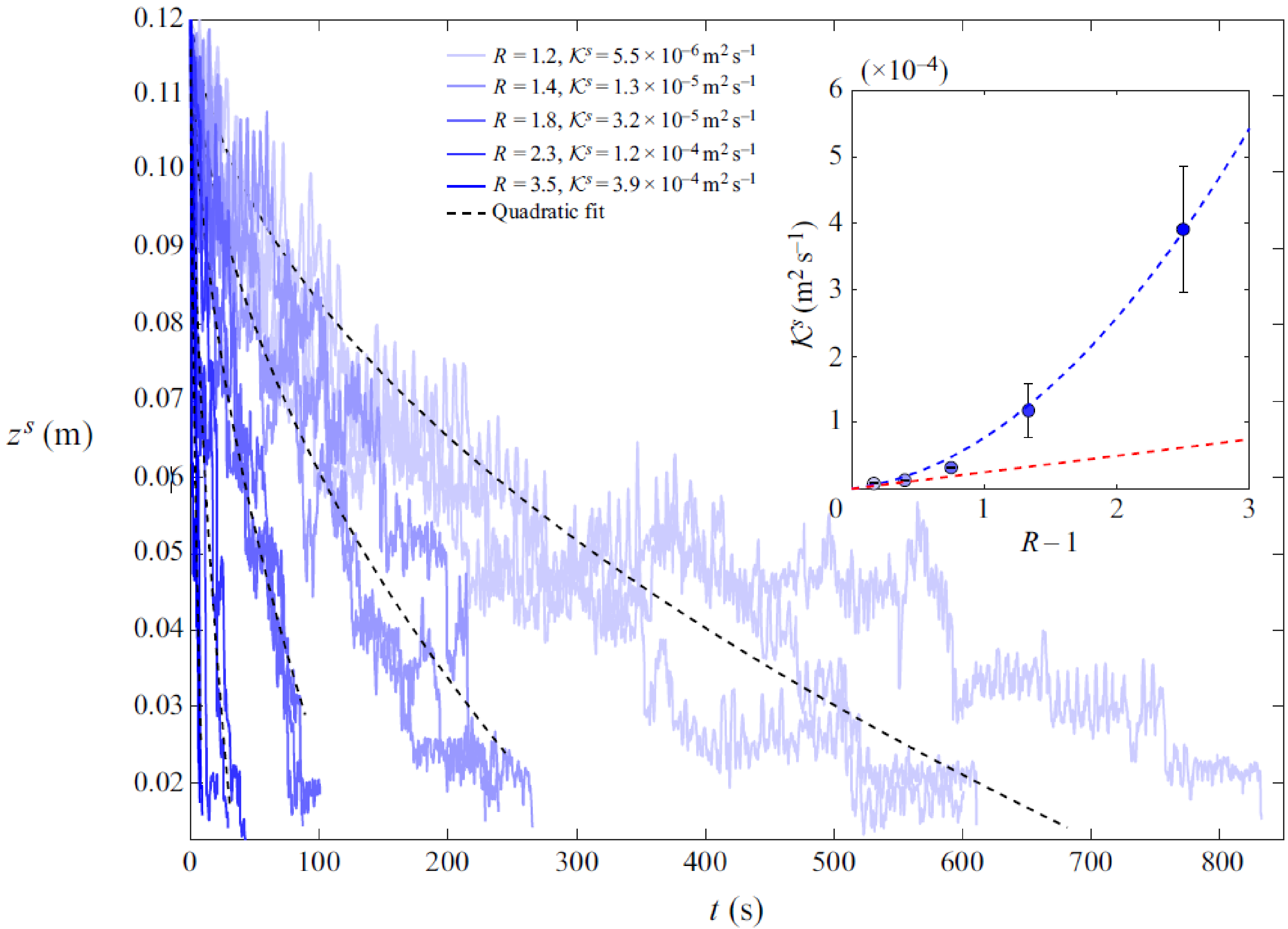

- For small R the small intruders also have a linear dependence.
- As R nears spontaneous percolation limit, the dependence becomes quadratic.

Collapse of the intruder data suggests

- the segregation velocity magnitude scales as

$$f_{sl} = \frac{2||\boldsymbol{D}||\mathcal{B}\rho_* g\bar{d}^2}{\mathcal{C}\rho_* g\bar{d} + p}\left[(R-1) + \mathcal{E}\phi^l (R-1)^2\right],$$

- $\mathcal{B}$, $\mathcal{C}$ & $\mathcal{E}$ are universal non-dimensional constants.

- This is linear in the shear rate $\dot{\gamma} = 2||\boldsymbol{D}||$,

- inversely proportional to the pressure p, where $\mathcal{C}$ is introduced to prevent a singularity when $p = 0$.

- linear in the gravity g,

- quadratic in the average grain-size $\bar{d} = \phi^l d^l + \phi^s d^s$,
  If average particle-size is larger $\Rightarrow$ particle-size segregation is faster

- linear in the grain-size ratio $R = d^l/d^s$ close to unity, with a quadratic dependence at low concentrations of fines at larger R.

Trewhela, Ancey & Gray (2021) *J. Fluid Mech.* **916**, A55.

Coupling I: bulk flow with prescribed segregation rate

- Mono-disperse partially regularized theory for bulk flow
- Calculate the resultant segregation with prescribed $f_{\nu\lambda}$ and $\mathcal{D}_{\nu\lambda}$

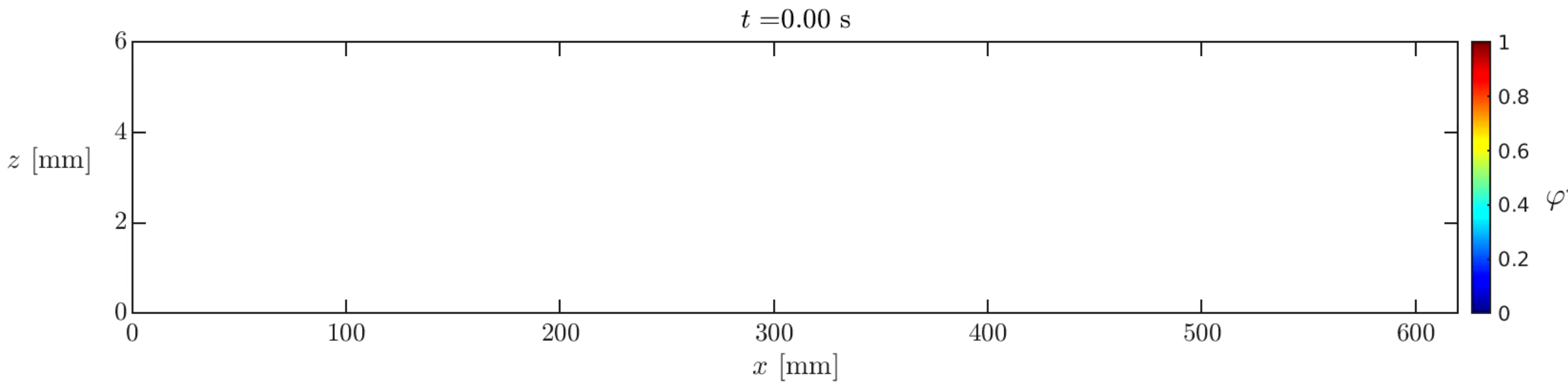

- A front propagates down the plane leaving a steady-uniform flow.
- 50:50 mixed inflow segregates to create diffuse layers with large particles on top of the fines (inverse grading).
- Large particles get preferentially transported to the front ...
- where they are over-run, but segregate upwards again and recirculate.
- $\Rightarrow$ large rich front + breaking size segregation wave

Barker, Rauter, Maguire, Johnson & Gray (2021) *J. Fluid Mech.* **909**, A22.
Thornton & Gray (2008) *J. Fluid Mech.* **596** 261–284

Coupling II: Segregation induced feedback on the bulk flow

- If the larger grains are more frictional than the fines then this can lead to the formation of a bulbous flow front

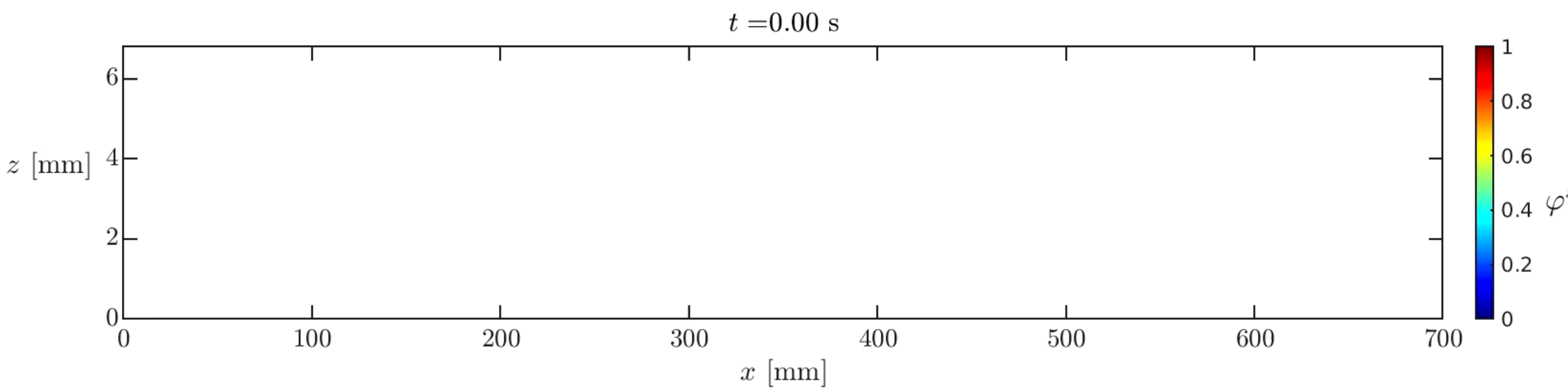

- arises through inertial number dependence on average particle size

$$I = \frac{2\bar{d}||\boldsymbol{D}||}{\sqrt{p/\rho_*}}, \quad \text{where} \quad \bar{d} = \sum_{\forall \nu} \phi^\nu d^\nu, \quad \text{higher } I \ \Rightarrow \ \text{greater friction}$$

- and different microscopic frictional properties of the particles

$$\bar{\mu} = \sum_{\forall \nu} \phi^\nu \mu^\nu.$$

Barker, Rauter, Maguire, Johnson & Gray (2021) *J. Fluid Mech.* **909**, A22.
Denissen *et al.* (2019) *J. Fluid Mech.* **866**, 263–297.

Bidisperse segregation in a triangular rotating drum

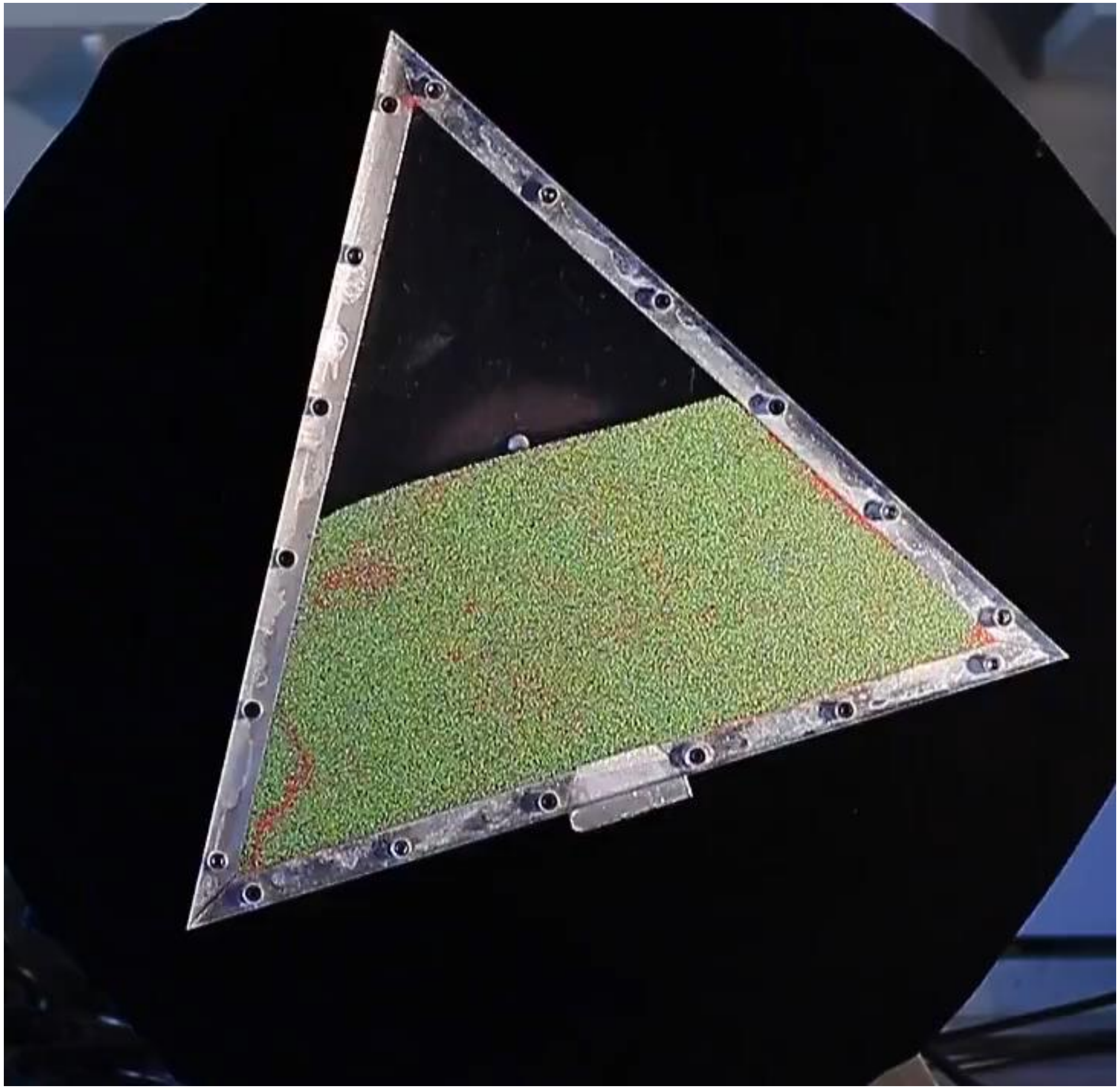

Maguire, Barker, Rauter, Johnson & Gray (2022) *J. Fluid Mech.* in prep.

Coupling III: Simulation in a triangular rotating drum

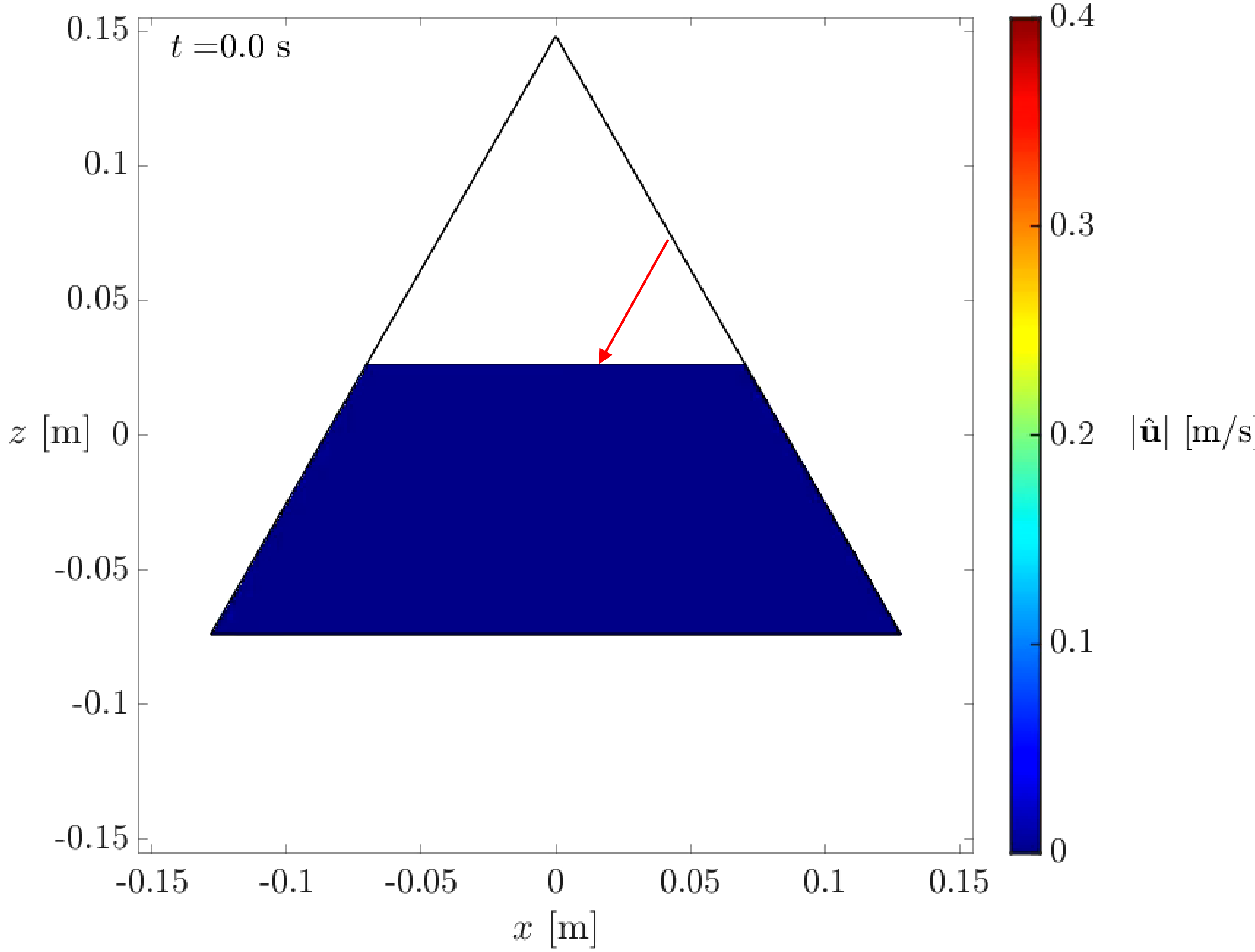

Maguire, Barker, Rauter, Johnson & Gray (2022) *J. Fluid Mech.* in prep.

Coupling III: Simulation in a triangular rotating drum

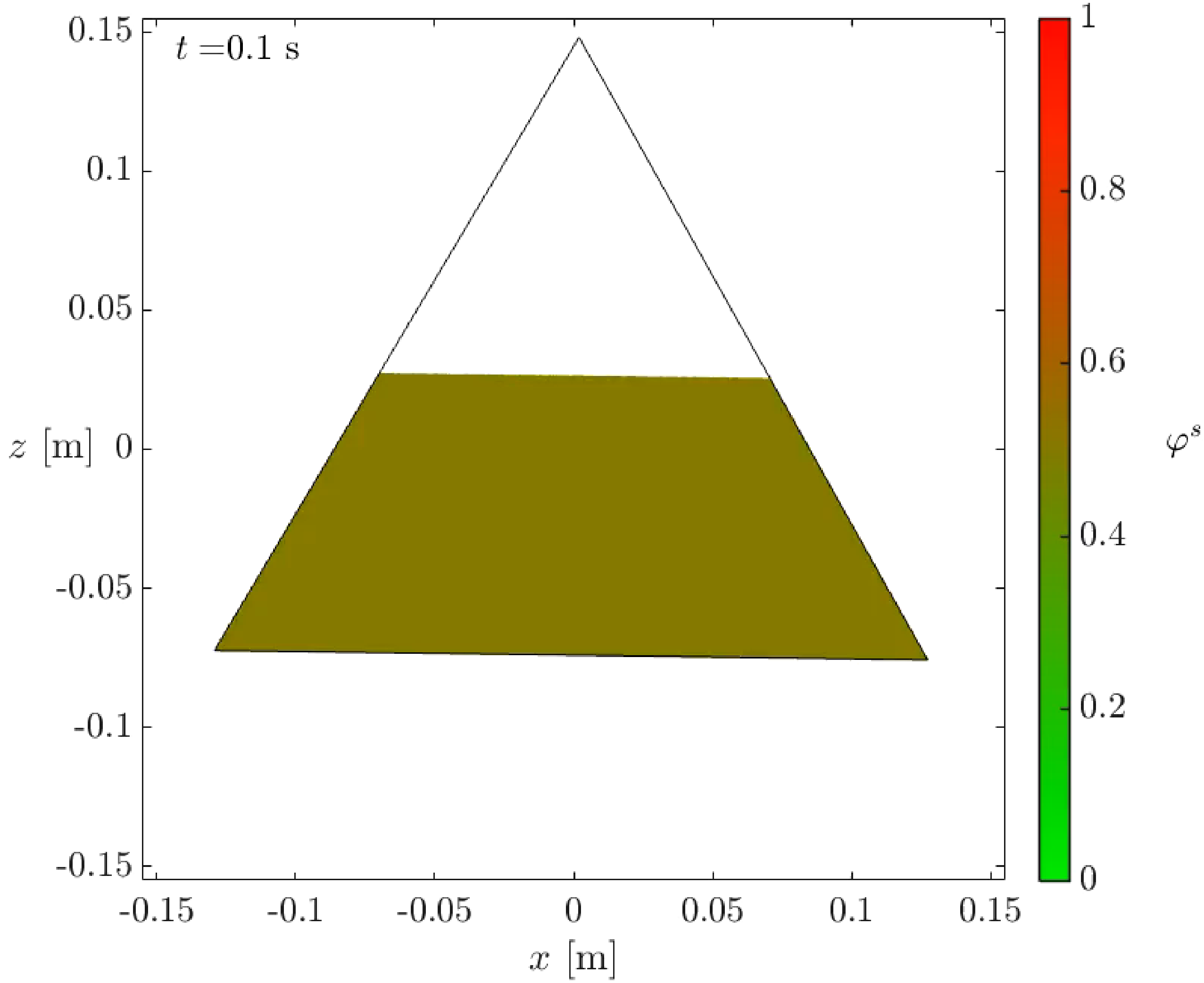

Maguire, Barker, Rauter, Johnson & Gray (2022) *J. Fluid Mech.* in prep.

Compressible / Dependent Rheology (CIDR)

Barker, Schaeffer, Shearer & Gray (2017) *Proc. Roy. Soc. A* **473**, 20160846.

Assuming ϕ is the solids volume fraction mass and momentum are

$$(\partial_t + u_j\partial_j)\phi + \phi \text{ div } \boldsymbol{u} = 0$$

$$\rho_*\phi(\partial_t + u_j\partial_j)u_i = -\partial_i p + \partial_j \tau_{ij} + \rho_*\phi g_i$$

Deviatoric strain-rate tensor

$$S_{ij} = \frac{1}{2}(\partial_j u_i + \partial_i u_j) - \frac{1}{2}(\text{div } \boldsymbol{u})\delta_{ij} \qquad D_{ij} = \frac{1}{2}(\partial_j u_i + \partial_i u_j)$$

Alignment: $\dfrac{S_{ij}}{\|\boldsymbol{S}\|} = \dfrac{\tau_{ij}}{\|\boldsymbol{\tau}\|}$ where $\|\boldsymbol{S}\| = \sqrt{S_{ij}S_{ij}/2}$

Yield Condition: $\|\boldsymbol{\tau}\| = Y(p, \phi, I)$ $\qquad \|\boldsymbol{\tau}\| = \mu(I)p$

Flow Rule: $\text{div}\,\boldsymbol{u} = 2f(p, \phi, I)\,\|\boldsymbol{S}\|$ $\qquad \text{div}\,\boldsymbol{u} = 0, \;\; f = 0$

Compressible I Dependent Rheology (CIDR)

Barker, Schaeffer, Shearer & Gray (2017) *Proc. Roy. Soc. A* **473**, 20160846.

The model is ALWAYS WELL-POSED provided

(i) $$\frac{\partial Y}{\partial p} - \frac{I}{2p}\frac{\partial Y}{\partial I} = f + I\frac{\partial f}{\partial I}$$

(ii) $$\frac{\partial Y}{\partial I} > 0$$

(iii) $$\frac{\partial f}{\partial p} - \frac{I}{2p}\frac{\partial f}{\partial I} < 0$$

.

• CIDR is a general framework for the formulation of well-posed models for granular flow.

• There are infinitely many well-posed models with different choices for the yield and dilatancy functions Y and f.

The $\mu(I)$-rheology [$Y = \mu(I)p$, $f = 0$] fails conditions (i) and (iii).

1/. The *μ(I),Φ(I)*-rheology and Inertial CIDR

Schaeffer, Barker, Gremaud, Shearer, Tsuji & Gray (2019) *J. Fluid Mech* submitted.

- The $\mu(I), \Phi(I)$-rheology has strict inertial number dependence

$$||\boldsymbol{\tau}|| = \mu(I)p, \qquad \phi = \Phi(I),$$

- The monotonic decrease of Φ allows it to be inverted to give

$$I = \Psi(\phi),$$

- The key idea of inertial CIDR is to introduce a yield function

$$Y(p, I, \phi) = \mu(\Psi(\phi))\frac{I}{\Psi(\phi)}p,$$

and dilatancy function

$$f(I, \phi) = \frac{1}{4}\mu(\Psi(\phi))\left[\frac{I}{\Psi(\phi)} - \frac{\Psi(\phi)}{I}\right],$$

that reduce to the $\mu(I), \Phi(I)$-rheology in steady-state isochoric (constant volume) flow, BUT ARE ALWAYS WELL POSED

The $\mu(I),\Phi(I)$-rheology and Inertial CIDR

Schaeffer, Barker, Tsuji, Gremaud, Shearer & Gray (2019) *J. Fluid Mech* **874**, 926–951

- Substituting the dilatancy function into the flow rule implies

$$I^2 - 2\frac{\Psi(\phi)\,\mathrm{div}\,\boldsymbol{u}}{\mu(\Psi(\phi))\,\|\boldsymbol{S}\|}I - \Psi(\phi)^2 = 0,$$

- Substituting the inertial number $I = 2d||\boldsymbol{S}||/\sqrt{p/\rho_*}$ implies

$$p = \rho_* \left(\frac{2d}{\mu(\Psi(\phi))\Psi(\phi)}\right)^2 \left[\sqrt{(\mathrm{div}\,\boldsymbol{u})^2 + \mu(\Psi)^2\|\boldsymbol{S}\|^2} - \mathrm{div}\,\boldsymbol{u}\right]^2,$$

which is well defined.

- The deviatoric shear stresses are also given explicitly as

$$\tau_{ij} = \frac{2d\sqrt{\rho_*}\mu(\Psi(\phi))}{\Psi(\phi)}\sqrt{p}\,S_{ij},$$

which is good for the development of numerical methods.

Simple shear simulations with *μ(I),Φ(I)*-rheology and Inertial CIDR

Schaeffer, Barker, Tsuji, Gremaud, Shearer & Gray (2019) *J. Fluid Mech* **874**, 926–951

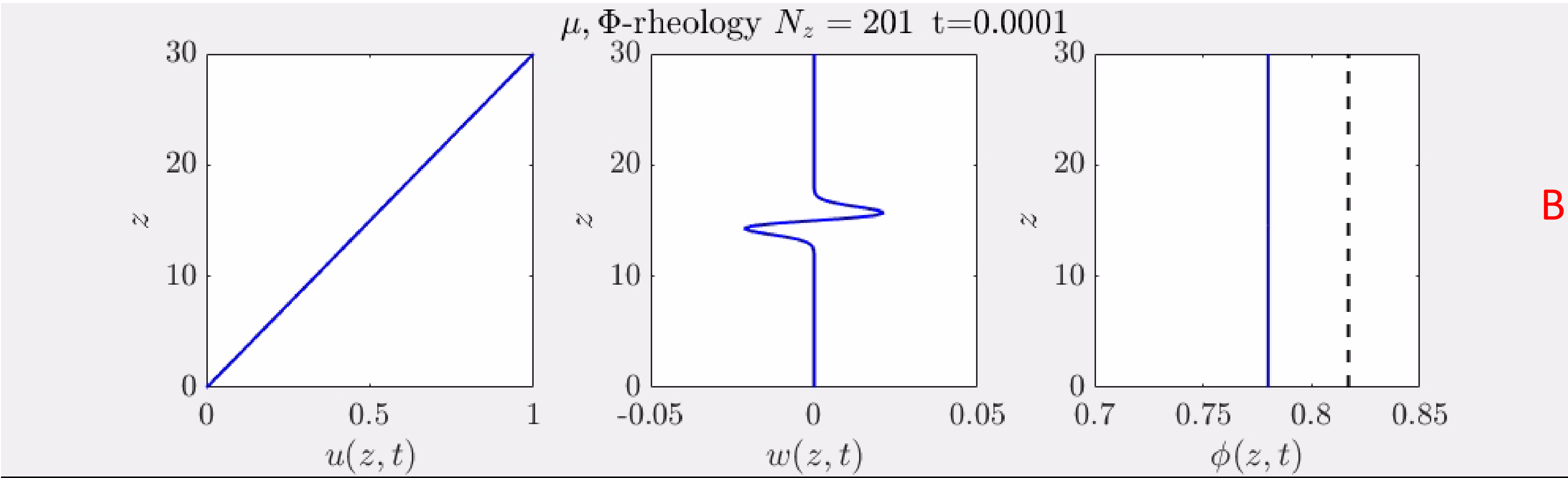

Blows up

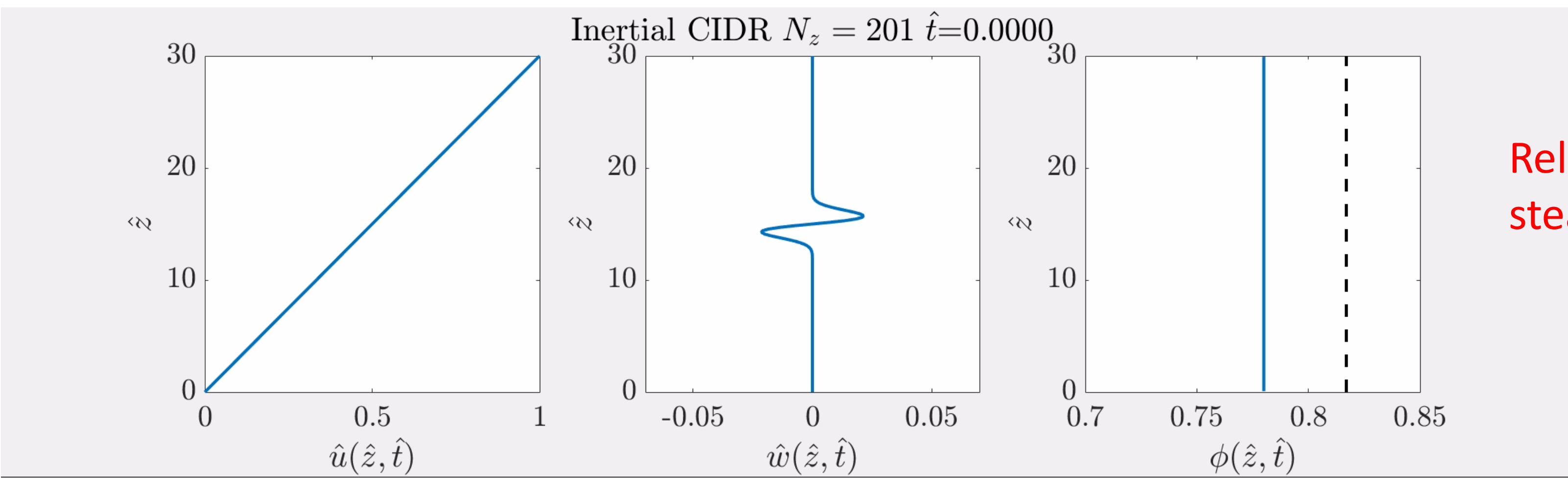

Relaxes to steady state

Simple shear simulations with inertial CIDR

Schaeffer, Barker, Tsuji, Gremaud, Shearer & Gray (2019) *J. Fluid Mech* **874**, 926–951

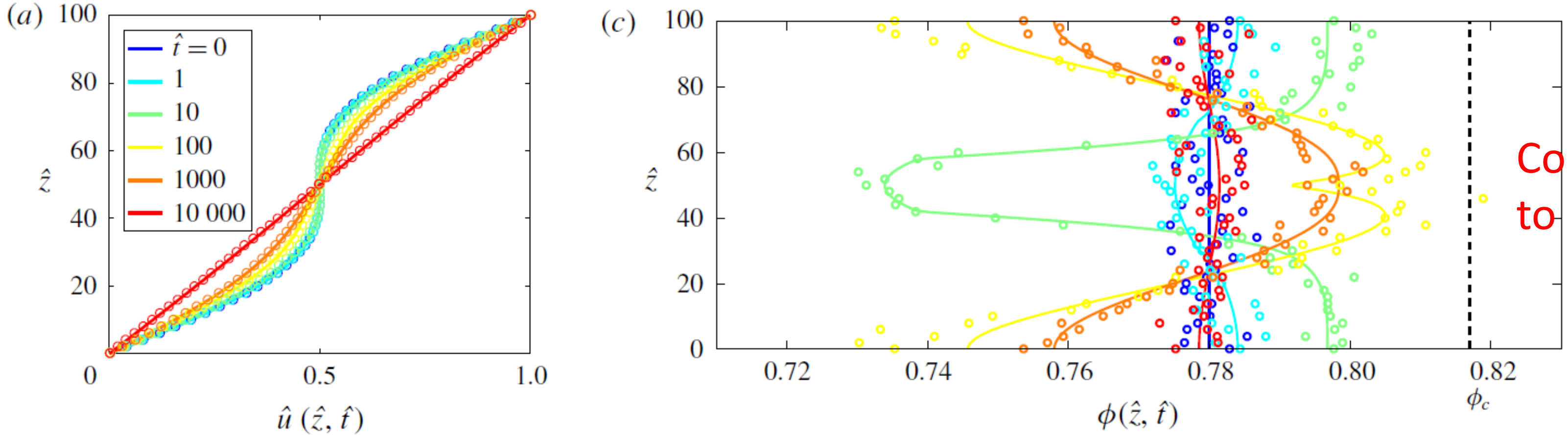

Comparison to DEM

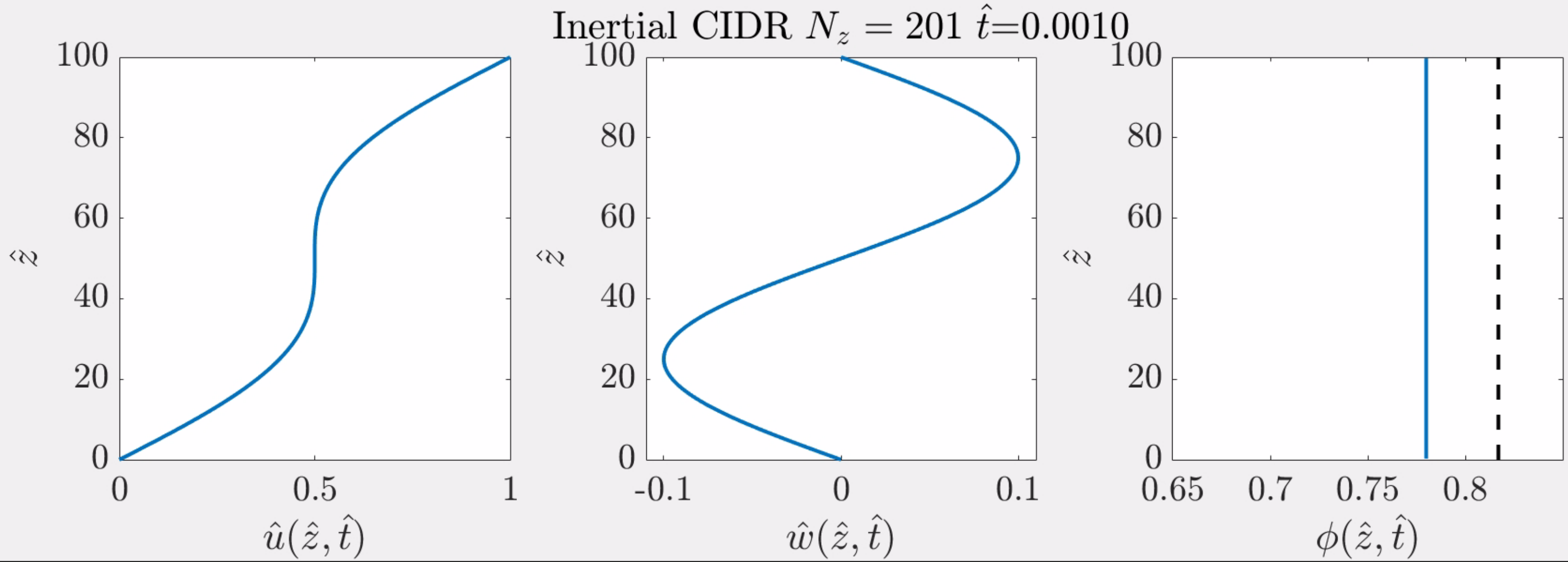

Critical State Soil Mechanics

Barker, Schaeffer, Shearer & Gray (2017) *Proc. Roy. Soc. A* **473**, 20160846.

This has a yield function and a dilatancy law of the form, e.g.

$$||\boldsymbol{\tau}|| = Y(p,\phi) = 2\mu p - \frac{p^2}{C(\phi)}, \qquad \operatorname{div}\boldsymbol{u} = 2\frac{\partial Y}{\partial p}(p,\phi)||\boldsymbol{S}||$$

Critical State line is where $\partial Y/\partial p = 0$ and hence where $||\boldsymbol{\tau}|| = \mu p$

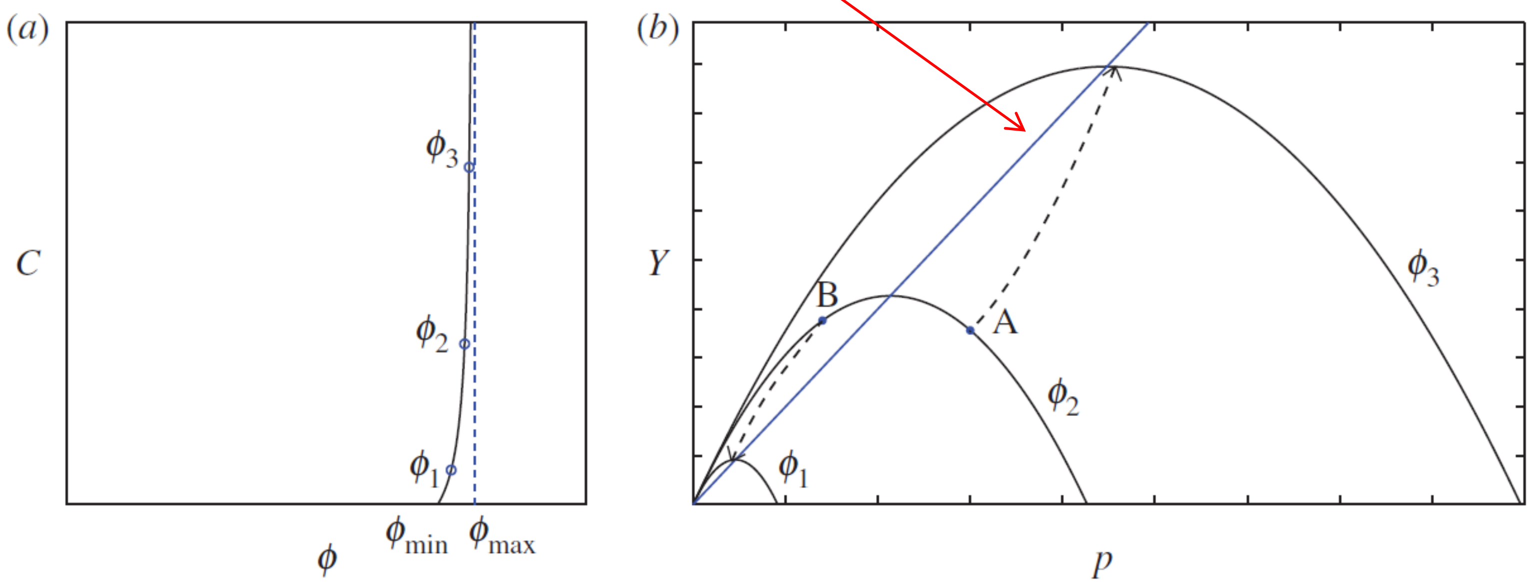

At A (B), $\partial_p Y < 0$, (> 0), so $\operatorname{div}\boldsymbol{u} < 0$, ($> 0$), the material compacts (expands) and the yield function grows (shrinks).

BUT fails the ill-posedness condition (ii)

2/. CSSM CIDR for solid-like deformations

Barker, Schaeffer, Shearer & Gray (2017) *Proc. Roy. Soc. A* **473**, 20160846.

The basic idea is to make the yield and dilatancy functions dependent on the inertial number e.g.

$$Y(p,\phi,I) = \alpha(I)p - \frac{p^2}{C(\phi)} \qquad f(p,\phi,I) = \beta(I) - \frac{2p}{C(\phi)}$$

These satisfy the well-posedness conditions (i)–(iii).

The functions $\alpha(I)$ and $\beta(I)$ can be chosen so that $\|\boldsymbol{\tau}\| = \mu(I)p$ for isochoric flow, i.e. the critical state line is I dependent.

CIDR therefore provides a very general framework for formulating well-posed granular flow models that span fluid-like and solid-like regimes.

Frictional hysteresis and the formation of h_{stop} and h_{start} layers

Daerr & Douady (1999) *Nature* **399**, 241–243.

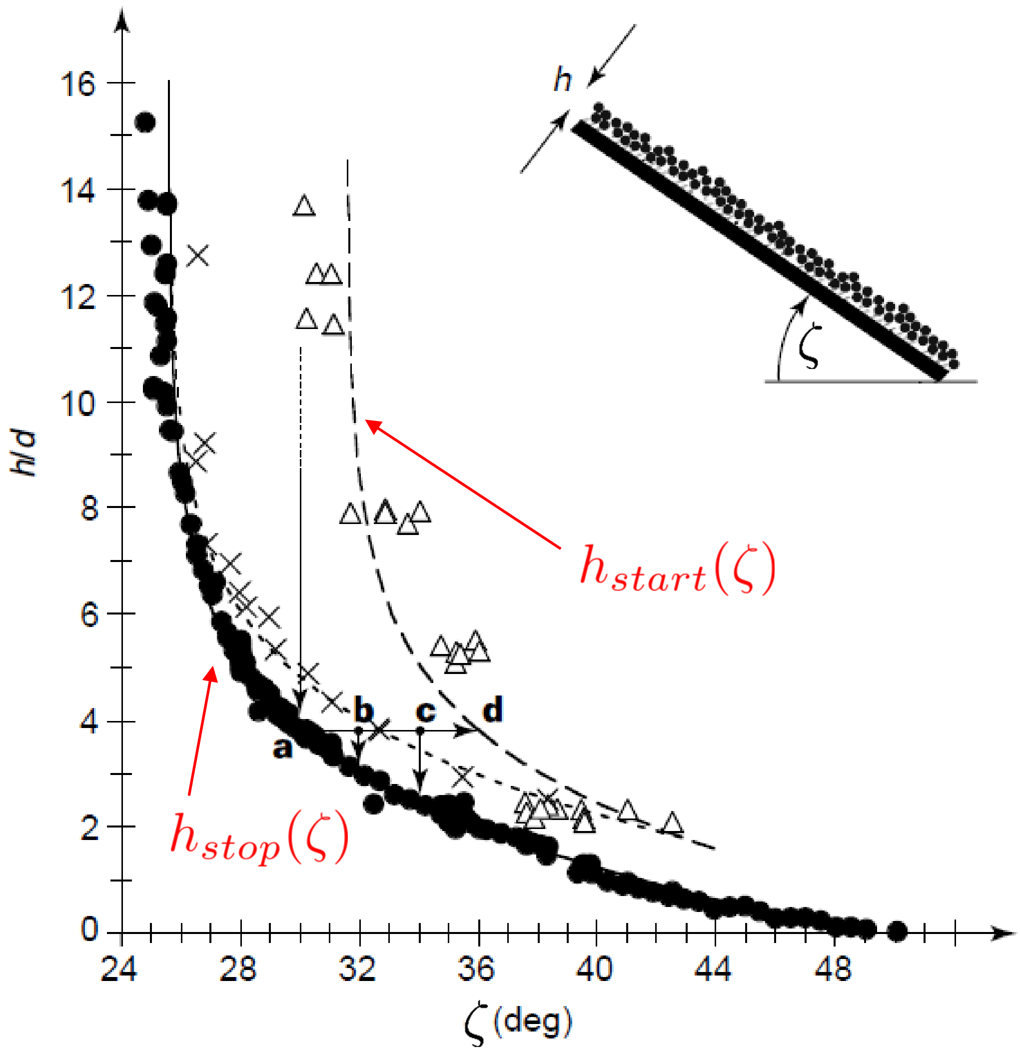

- On a rigid rough bed at an angle ζ, a steady-uniform granular flow will leave behind a layer of thickness $h_{stop}(\zeta)$ when it comes to rest.
- This relation can be inverted to determine $\zeta = \zeta_{stop}(h)$
- The deposit will not be remobilized unless $\zeta_{start}(h) > \zeta_{stop}(h)$

The h_{stop} and h_{start} can be used to determine the friction μ

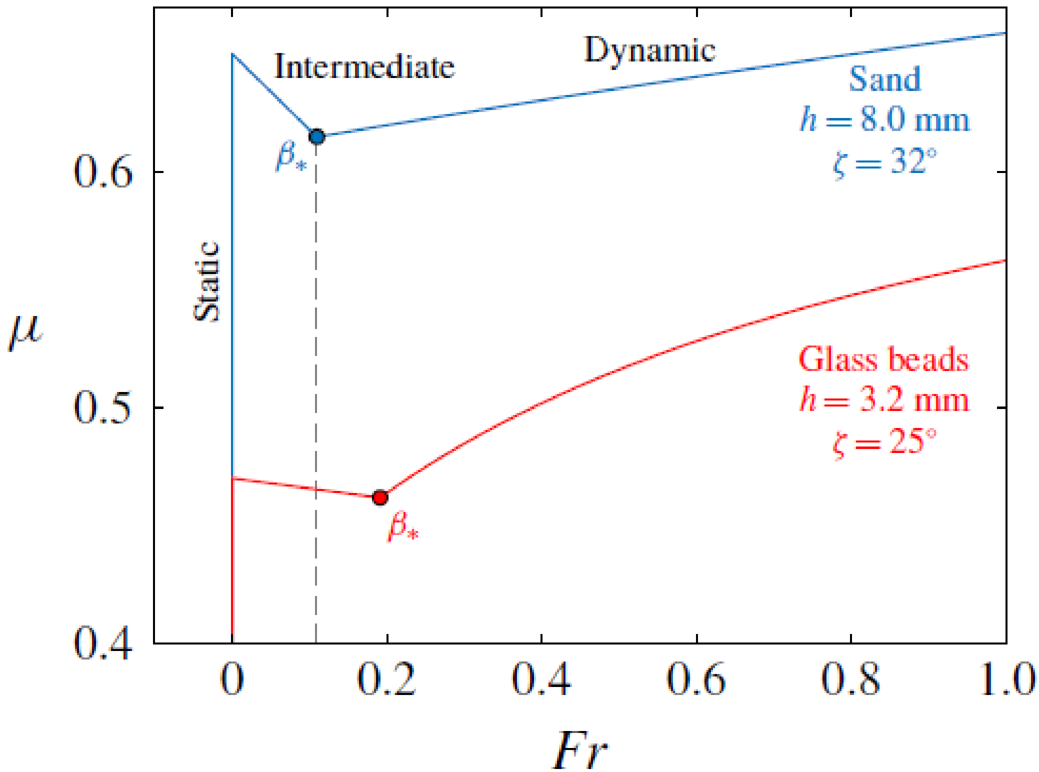

$$Fr = \frac{\bar{u}}{\sqrt{hg\cos\zeta}}$$

$$\mu_b(h, Fr) = \begin{cases} \mu_D, & Fr \geq \beta_*, \\ \mu_I, & 0 < Fr < \beta_*, \\ \mu_S, & Fr = 0, \end{cases}$$

- Measurement of the depth-averaged steady-uniform velocity $\bar{u}$ as a function of flow depth h together with $h_{stop}(\zeta)$ and $h_{start}(\zeta)$ are sufficient to determine a non-monotonic friction $\mu = \mu(h, Fr)$ that is a function of h and the Froude number Fr.

Pouiquen (1999) *Phys. Fluids* **11**(3), 542–548.
Pouliquen & Forterre (2002) *J. Fluid Mech.* **453**, 133-151.
Edwards *et al.* (2019) *J. Fluid Mech.* **875**, 1058–1095.

Monodisperse leveed channels 160-200 μm

Félix & Thomas (2004) *Earth & Planetary Sci. Lett.* **221**, 197–213.
Deboeuf *et al.* (2006) *Phys. Rev. Lett.* **97**, 158303.
Takagi, McElwaine & Huppert (2011) *Phys. Rev. E* **83**(3), 031306.

Depth-averaged models incorporating hysteresis and viscosity

- For avalanche thickness h and depth-averaged velocity $\bar{\boldsymbol{u}}$ the depth-averaged mass and momentum balances are

(i) well-posed granular fingering
(ii) roll wave high frequency cut-off
(iii) velocity profiles across channels

$$\frac{\partial h}{\partial t} + \mathrm{div}(h\bar{\boldsymbol{u}}) = 0,$$

$$\frac{\partial}{\partial t}(h\bar{u}) + \mathrm{div}(h\bar{\boldsymbol{u}} \otimes \bar{\boldsymbol{u}}) + \mathrm{grad}\left(\frac{1}{2}h^2 g\cos\zeta\right) = hg\boldsymbol{S}\cos\zeta + \boxed{\mathrm{div}\left(\nu h^{\frac{3}{2}}\overline{\boldsymbol{D}}\right)},$$

- source terms composed of gravity and basal friction

$$\boldsymbol{S} = \begin{pmatrix} \tan\zeta - \mu\, e_1, \\ -\mu\, e_2, \end{pmatrix}, \qquad \boldsymbol{e} = (e_1, e_2) = \begin{cases} \dfrac{\bar{\boldsymbol{u}}}{|\bar{\boldsymbol{u}}|}, & |\bar{\boldsymbol{u}}| > 0, \\ \dfrac{\tan\zeta\boldsymbol{i} - \nabla h}{|\tan\zeta\boldsymbol{i} - \nabla h|}, & |\bar{\boldsymbol{u}}| = 0, \end{cases}$$

- The two-dimensional strain-rate tensor is

$$\overline{\boldsymbol{D}} = \frac{1}{2}\left(\nabla\bar{\boldsymbol{u}} + \nabla\bar{\boldsymbol{u}}^T\right)$$

- the coefficient ν in the viscosity $\nu h^{1/2}/2$ is determined from $\mu(I)$-rheology

Gray & Edwards (2014), J. Fluid Mech. **755**, 503–534.
Baker, Barker & Gray (2016) *J. Fluid Mech.* **787**, 367-395.
Baker, Johnson & Gray *J. Fluid Mech.* **809**, 168–212.
Rocha, Johnson & Gray (2019) *J. Fluid Mech.* **876**, 591–641.
Edwards *et al.* (2021) *J. Fluid Mech.* **915**, A9.

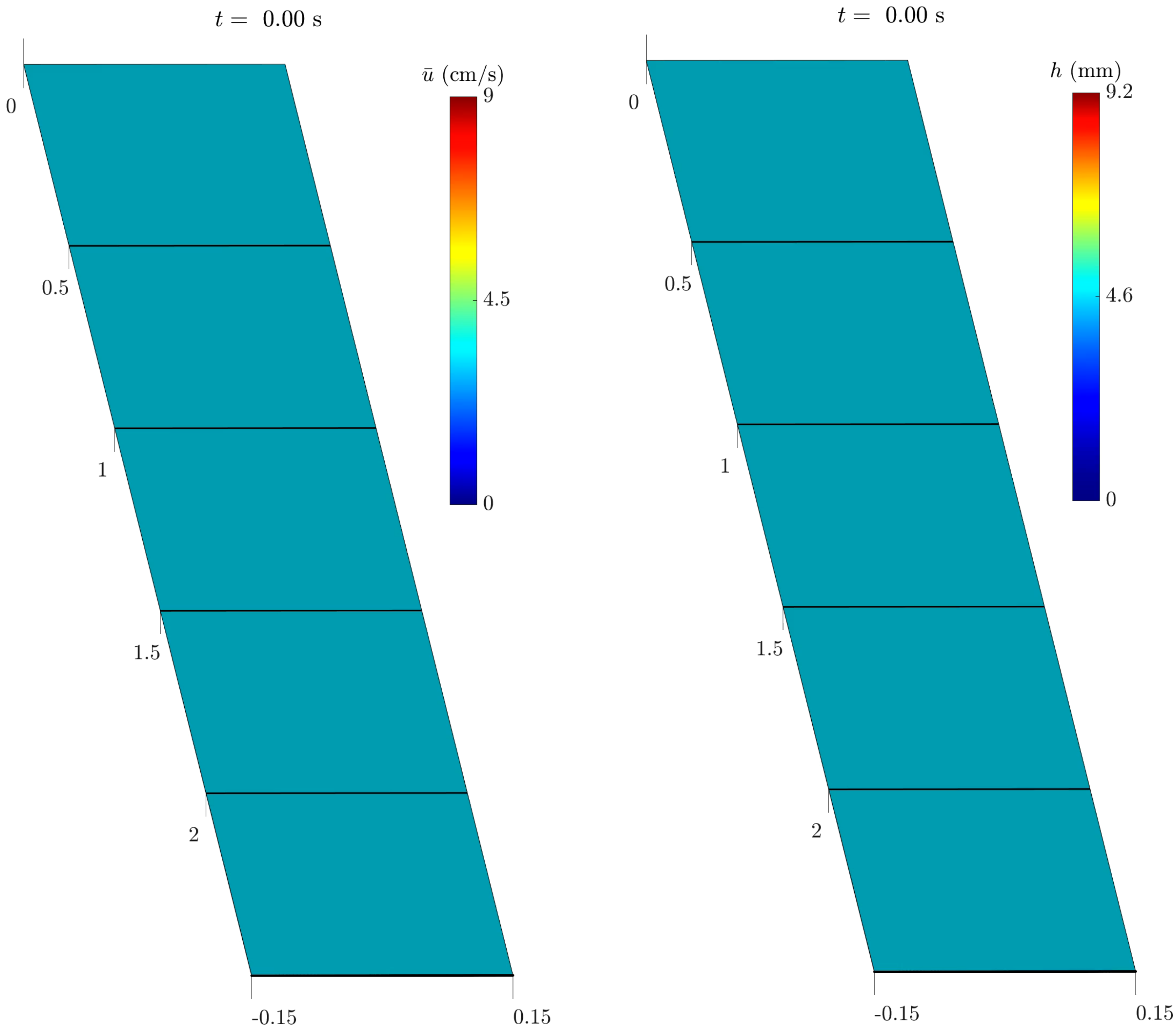

Rocha, Johnson & Gray (2019) *J. Fluid Mech.* **876**, 591–641.

Comparison to experiments of Takagi *et al.* (2011)

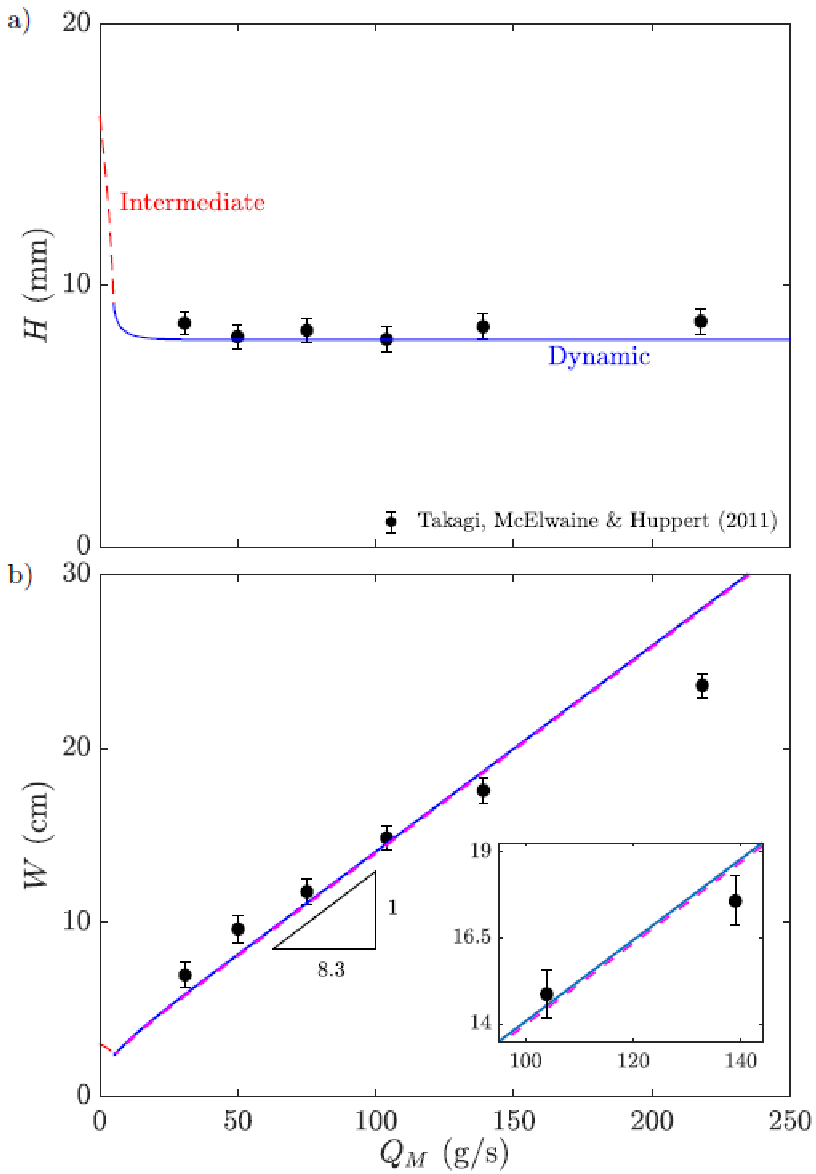

- The avalanche thickness H is almost constant with Q_M
- but this thickness is significantly deeper than $h_{stop} = 5$ mm
- The width W increases linearly with the mass flux Q_M
- but below a critical mass flux the solutions become unstable

Takagi, McElwaine & Huppert (2011) *Phys. Rev. E* **83**, 031306.
Rocha, Johnson & Gray (2019) *J. Fluid Mech.* **876**, 591–641.

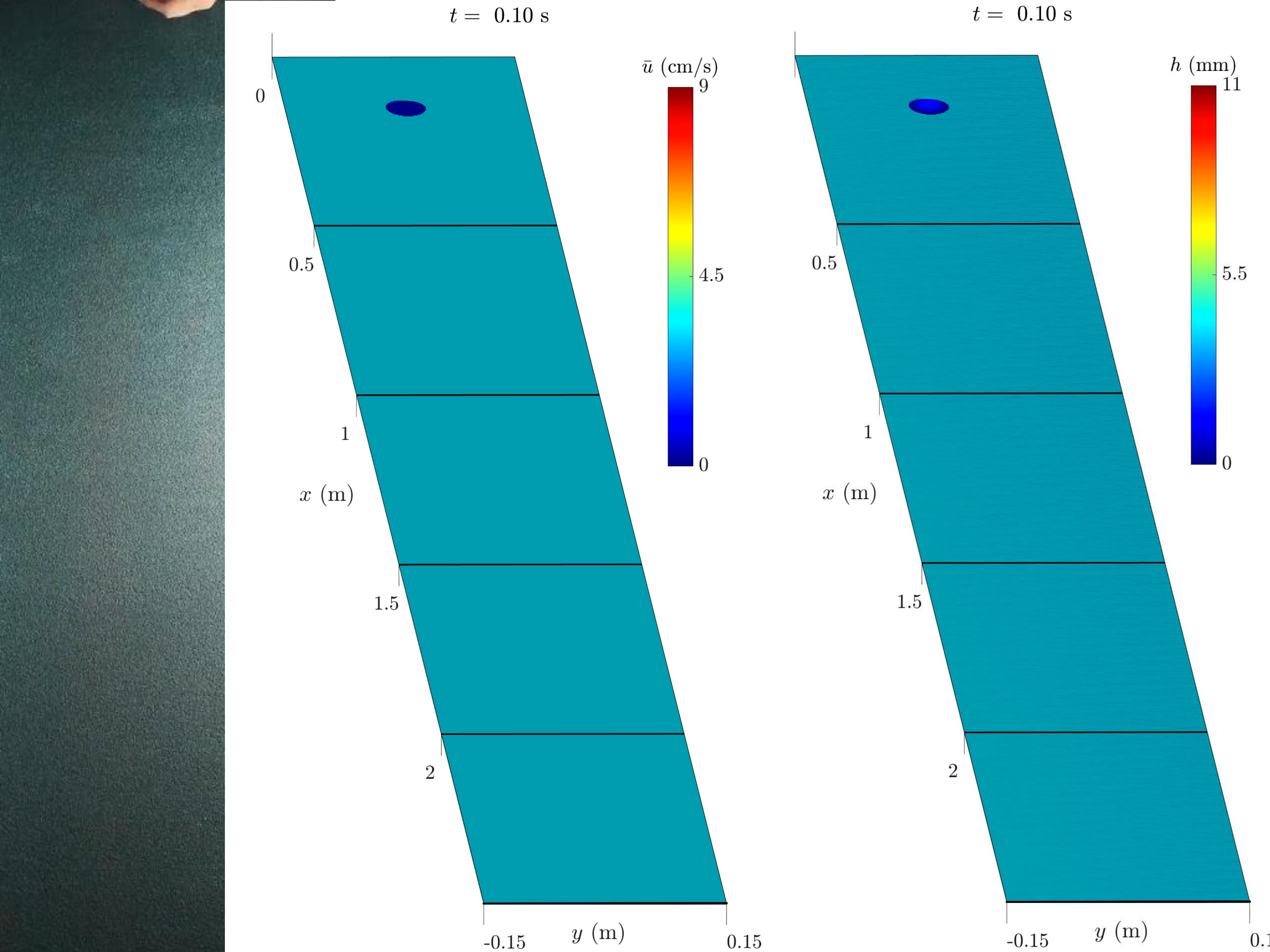

t = 0.10 s
ū (cm/s)
9
4.5
0
0
0.5
1
1.5
2
x (m)
y (m)
-0.15
0.15
t = 0.10 s
h (mm)
11
5.5
0
0
0.5
1
1.5
2
x (m)
y (m)
-0.15

Erosion-deposition waves on an erodible bed of red sand

All yellow sand particles are deposited ... avalanche propagates as a wave

Edwards, Viroulet, Johnson & Gray (2021) *J. Fluid Mech.* **915**, A9.

Summary and conclusions

- The $\mu(I)$ rheology has the potential to model many industrial flows.
- It needs more frictional parameters. Industry will need to adopt new tests to measure these, e.g. inclined chute flows.
- Application to transient problems can lead to grid dependent results due to ill-posedness (unbounded short-wave-length instabilities).
- The worst effects can be removed by modifying the $\mu = \mu(I)$ function.
- This allows coupling with segregation models to compute the evolving particle-size distribution in flows of practical interest.
- Compressibility can generate granular theories that are always well-posed, and with the same steady-state response as the $\mu(I)$-rheology. General numerical methods still need to be developed to solve these 'Compressible I-dependent rheologies' (CIDR).
- Non-local effects that can not be modelled with such theores, and additional fields need to be incorprated, e.g. fluidity or granular temperature.
- Relatively simple depth-averaged models are making progress in capturing frictional hysteresis and the h_{stop} and h_{start} phenomenolgy.